

WL-TR-97-4088



SPECTRUM AND STRUCTURE OF SPIROPYRAN

J. A. YOUNG  
B. L. FARMER  
DEPARTMENT OF MATERIALS SCIENCE AND ENGINEERING  
UNIVERSITY OF VIRGINIA  
CHARLOTTESVILLE, VA 22903-2442

W. W. ADAMS  
MATERIALS DIRECTORATE  
WRIGHT LABORATORY, AFMC  
WRIGHT-PATTERSON AFB, OH 45433-7702

AUGUST 1994

FINAL REPORT FOR PERIOD 1 SEPTEMBER 1992 - 15 AUGUST 1994

APPROVED FOR PUBLIC RELEASE, DISTRIBUTION UNLIMITED.

DTIC QUALITY INSPECTED 2

MATERIALS DIRECTORATE  
WRIGHT LABORATORY  
AIR FORCE MATERIEL COMMAND  
WRIGHT-PATTERSON AFB, OH 45433-7734

19971222 014

## NOTICE

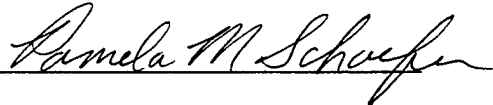
When Government drawings, specifications, or other data are used for any purpose other than in connection with a definitely Government-related procurement, the United States Government incurs no responsibility or any obligation whatsoever. The fact that the Government may have formulated or in any way supplied the said drawings, specifications, or other data, is not to be regarded by implication, or otherwise in any manner construed, as licensing the holder, or any other person or corporation; or as conveying any rights or permission to manufacture, use, or sell any patented invention that may in any way be related thereto.

This report is releasable to the National Technical Information Service (NTIS). At NTIS, it will be available to the general public, including foreign nations.

This technical report has been reviewed and is approved for publication.



W. WADE ADAMS  
Hardened Materials Technology Section  
Hardened Materials Branch



PAMELA SCHAEFER, Chief  
Hardened Materials Branch  
Electromagnetic Materials and  
Survivability Division



WILLIAM R. WOODY, Chief  
Electromagnetic Materials and  
Survivability Division

If your address has changed, if you wish to be removed from our mailing list, or if the addressee is no longer employed by your organization please notify WL/MLPJ, Wright-Patterson AFB, OH 45433-7702 to help maintain a current mailing list.

Copies of this report should not be returned unless return is required by security considerations, contractual obligations, or notice on a specific document.

|   |  |   |   |  |
|---|--|---|---|--|
| <b>REPORT DOCUMENTATION PAGE</b>  |  |   | FORM APPROVED<br>OMB NO. 0704-0188  |  |
| Public reporting burden for this collection of information is estimated to average .hour per response, including the time for reviewing instructions, searching existing data sources, gathering and maintaining the data needed, the complete and review the collection of information. Send comments regarding this burden estimate or any other aspects of this collection of information, including suggestions and reducing this burden to Washington Headquarters Services, Directorate for Information Operations and Reports, 1215 Jefferson Davis Highway, Suite 1204, Arlington, VA 22202-4302, and to the Office of Management and Budget, Paperwork Reduction Project (08704-0188), Washington, DC 20503.   |  |   |   |  |
| 1. AGENCY USE ONLY (Leave Blank)  |  | 2. REPORT DATE<br>August 1994                       |   | 3. REPORT TYPE AND DATES COVERED<br>Final Report 1 Sept 92 - 15 Aug 94 |
| 4. TITLE AND SUBTITLE<br>Spectrum and Structure of Spiropyran   |  |   | 5. FUNDING NUMBERS<br><br>C: F33615-92-D-5000<br>PE: 63112F<br>PA: 4SU1<br>TA: 04<br>WU: 57 |  |
| 6. AUTHOR(S)<br>J. A. Young<br>B. L. Farmer<br>W. W. Adams  |  |   |   |  |
| 7. PERFORMING ORGANIZATION NAME(S) AND ADDRESS(ES)<br>University of Virginia<br>Department of Materials Science and Engineering<br>Charlottesville, VA 22903-2442<br>Materials Directorate<br>Wright Laboratory, AFMC<br>Wright-Patterson AFB, OH<br>45433-7702   |  |   | 8. PERFORMING ORGANIZATION<br>REPORT NUMBER   |  |
| 9. SPONSORING MONITORING AGENCY NAME(S) AND ADDRESS(ES)<br>Materials Directorate<br>Wright Laboratory<br>Air Force Materiel Command<br>Wright-Patterson AFB OH 45433-7734<br>POC: John Eric, WL/MLPJ, 937-255-3808 ext 3165   |  |   | 10. SPONSORING/MONITORING<br>AGENCY REP NUMBER<br><br>WL-TR-97-4088                         |  |
| 11. SUPPLEMENTARY NOTES   |  |   |   |  |
| 12a. DISTRIBUTION/AVAILABILITY STATEMENT<br><br>Approved for public release; distribution unlimited.  |  |   | 12b. DISTRIBUTION CODE  |  |
| 13. ABSTRACT<br><p>Photochromic materials are of interest to the Air Force for a variety of potential applications including high resolution photography, optical devices, holographic systems and variable transmission devices.</p> <p>The photochemical and structural characteristics of two organic photochromes, specifically indoline-spiro-benzopyran and benzothiazoline-spiro-benzopyran, have been studied by computational chemistry techniques. Both quantum mechanical and classical methods were used. Irradiation of spiropyran by UV light causes molecular rearrangement, thus yielding merocyanine whose absorption band lies in the visible region. This is the basis of the photochromic nature of the spiropyran. Several chromophore based devices would benefit from a material whose visible absorption spectrum was red shifted and whose structure and properties in various environments was fully understood.</p> <p>The absorption spectra of both indoline-spiro-benzopyran and benzothiazoline-spiro-benzopyran were calculated. Spectroscopic calculations reveal that the absorption spectrum is determined by two factors: the choice of substituent and the geometry of the chromophore. Both electron withdrawing and electron donating substituents were strategically placed on the chromophore. Maximum red shifts may be achieved in the merocyanine by attaching (at the proper position) strongly electron donating substituents which force rotations about double bonds while limiting the rotation about single bonds.</p> <p>Two force fields have been developed to allow classical calculations on large photochromic systems (solvated chromophores or polymer substituted chromophores). The agreement of these classical force fields with quantum mechanical methods for the unsubstituted indoline-benzopyran merocyanine has been shown. These force fields were used in molecular dynamics simulations to explore the effect of the solvent polarity on the chromophore. The calculations demonstrated the ability of polar solvents to stabilize the merocyanine form, thus potentially reducing the fading rate of the chromophore.</p> |  |   |   |  |
| 14. SUBJECT TERMS<br>photochromes<br>spiropyran<br>merocyanine  |  |   | 15. NUMBER OF PAGES<br>73   |  |
| computational chemistry<br>quantum mechanical methods<br>molecular dynamics simulations   |  |   | 16. PRICE CODE  |  |
| 17. SECURITY CLASSIFICATION<br>OF REPORT<br>UNCLASSIFIED  |  | 18. SECURITY CLASS<br>OF THIS PAGE.<br>UNCLASSIFIED |   | 19. SECURITY CLASS<br>OF ABSTRACT<br>UNCLASSIFIED                      |
| 20. LIMITATION ABSTRACT<br>SAR  |  |   |   |  |

# TABLE OF CONTENTS

| <u>SECTION</u>                                 | <u>PAGE</u> |
|--|-------------|
| I. <u>INTRODUCTION</u>                         | 1           |
| 1.1. Motivation                                | 1           |
| 1.2. Photochromism                             | 2           |
| 1.3. Factors Influencing Photochromism         | 6           |
| 1.4. Technological Applications                | 7           |
| 1.5. Approach                                  | 8           |
| II. <u>THEORY</u>                              | 10          |
| 2.1. Quantum Mechanics                         | 10          |
| 2.1.1. LCAO/SCF Method                         | 11          |
| 2.1.2. Configuration Interaction               | 13          |
| 2.2. Classical Mechanics                       | 15          |
| 2.2.1. Molecular Mechanics                     | 17          |
| 2.2.2. Molecular Dynamics                      | 17          |
| III. <u>RESULTS AND DISCUSSION</u>             | 19          |
| 3.1. Spectroscopic Modeling                    | 19          |
| 3.1.1. Methodology                             | 20          |
| 3.1.2. Unsubstituted Indoline-Spiro-Benzopyran | 22          |
| 3.1.3. Spectral Shifts                         | 34          |
| 3.1.4. The Benzothiazoline-Benzopyran          | 46          |
| 3.2. Force Field Modeling                      | 50          |
| 3.2.1. Force Field Parameterization            | 50          |

## TABLE OF CONTENTS (con't)

|                                      |    |
|--------------------------------------|----|
| 3.2.2. Molecular Dynamics            | 63 |
| IV <u>CONCLUSION</u>                 | 67 |
| 4.1. Conclusion and Future Direction | 67 |
| V <u>REFERENCES</u>                  | 70 |

## LIST OF FIGURES

|              |  |    |
|--------------|--|----|
| Figure 1.1:  | Photochromism yields the apolar quinonic form and dipolar zwitterion form, respectively. | 4  |
| Figure 1.2:  | The indoline-spiro-benzopyran.   | 5  |
| Figure 1.3:  | The benzothiazoline-spiro-benzopyran.  | 5  |
| Figure 3.1:  | The experimental (curve) and calculated (spikes) spectra of naphthalene.                 | 21 |
| Figure 3.2:  | The indoline-spiro-benzopyran.   | 23 |
| Figure 3.3:  | The trans-cis indoline-benzopyran merocyanine.   | 24 |
| Figure 3.4:  | The cis-cis indoline-benzopyran merocyanine.   | 24 |
| Figure 3.5:  | The trans-trans indoline-benzopyran merocyanine.   | 25 |
| Figure 3.6:  | The cis-trans indoline-benzopyran merocyanine.   | 25 |
| Figure 3.7:  | A side view of the planar merocyanine.   | 26 |
| Figure 3.8:  | The experimental spectrum of the indoline-spiro-benzopyran.                              | 28 |
| Figure 3.9:  | The calculated spectrum of the indoline-spiro-benzopyran.                                | 28 |
| Figure 3.10: | The HOMO (g) of the indoline-spiro-benzopyran.   | 29 |
| Figure 3.11: | The LUMO (1) of the indoline-spiro-benzopyran.   | 29 |
| Figure 3.12: | The fifth unoccupied orbital (5) of the indoline-spiro-benzopyran.                       | 30 |

## LIST OF FIGURES (con't)

|              |   |    |
|--------------|---|----|
| Figure 3.13: | The experimental spectrum of the indoline-benzopyran merocyanine.   | 32 |
| Figure 3.14: | The calculated spectrum of the indoline-benzopyran merocyanine.   | 32 |
| Figure 3.15: | The HOMO of the indoline-benzopyran merocyanine.  | 33 |
| Figure 3.16: | The LUMO of the indoline-benzopyran merocyanine.  | 33 |
| Figure 3.17: | The numbering of the indoline-benzopyran merocyanine.   | 36 |
| Figure 3.18: | The computed spectra of the Cl substituted and unsubstituted indoline-benzopyran merocyanine.               | 38 |
| Figure 3.19: | The calculated spectra of substituted (H, OCH <sub>3</sub> and thiophene) indoline-benzopyran merocyanines. | 41 |
| Figure 3.20: | Spectra of substituted (H, OCH <sub>3</sub> and thiophene) indoline-spiro-benzopyrans.                      | 45 |
| Figure 3.21: | The numbering of the benthiozoline-benzopyran.  | 47 |
| Figure 3.22: | The spectra of substituted (H, OCH <sub>3</sub> and thiophene) trans-cis benzothiazoline-benzopyrans.       | 49 |
| Figure 3.23: | Potential energy surface of the merocyanine. $\phi_2 = 180^\circ$ .   | 52 |
| Figure 3.24: | Potential energy surface of the merocyanine. $\phi_1 = 0^\circ$ .   | 52 |
| Figure 3.25: | Bond order surface of bond one. $\phi_2 = 180^\circ$ .  | 54 |
| Figure 3.26: | Bond order surface of bond two. $\phi_2 = 180^\circ$ .  | 54 |
| Figure 3.27: | Bond order surface of bond three. $\phi_2 = 180^\circ$ .  | 55 |

## LIST OF FIGURES (con't)

|              |  |    |
|--------------|--|----|
| Figure 3.28: | Bond orders of bond 1, 2 and 3. $\phi_1=\phi_3=0^\circ$ .                          | 57 |
| Figure 3.29: | Comparison of the energies calculated by the modified 2-1-2 force field and MOPAC. | 59 |
| Figure 3.30: | Bond orders of bond 1, 2 and 3. $\phi_1=90^\circ$ and $\phi_2=180^\circ$ .         | 61 |
| Figure 3.31: | Comparison of the energies calculated by the 1-2-1 force field and MOPAC.          | 61 |
| Figure 3.32: | The indoline-benzopyran in water.  | 65 |
| Figure 3.33: | The stability of the merocyanine in various solvents.                              | 66 |



## LIST OF TABLES

|             |  |    |
|-------------|--|----|
| Table 3.1:  | Computed heats of formation of the indoline-benzopyran.  | 22 |
| Table 3.2:  | The effects of substituents on the absorption spectra.   | 35 |
| Table 3.3:  | The effects of geometry on the absorption spectra.   | 35 |
| Table 3.4:  | $\Delta P_{ij}$ values of the indoline-benzopyran merocyanine.   | 37 |
| Table 3.5:  | Torsion angles of electron withdrawing substituted merocyanine.  | 39 |
| Table 3.6:  | The torsions of substituted trans-cis indoline-benzopyran merocyanines.  | 40 |
| Table 3.7:  | Heats of formation of the substituted indoline-benzopyran isomers.   | 42 |
| Table 3.8:  | The torsions of substituted cis-cis indoline-benzopyran merocyanines. The torsions of the trans-cis isomer are shown in parentheses. | 43 |
| Table 3.9:  | $\Delta P_{ij}$ values for the benthiozoline-benzopyran.   | 48 |
| Table 3.10: | Modified TRIPOS 2-1-2 force field parameters. Values in parentheses are the original TRIPOS values.                                  | 57 |
| Table 3.11: | Modified TRIPOS 1-2-1 force field parameters. Values in parentheses are the original TRIPOS values.                                  | 58 |

## FOREWORD

This report was prepared under delivery number 30-2 of the Special Advanced Studies Hardened Materials program, contract F33615-92-D-5000, with Lawrence Associates, Inc., through a subcontract with the University of Virginia, Department of Materials Science and Engineering. The work was initiated under Project 2422, "Laser Hardened Materials", Task 0401, Work Unit Directive (WUD) 26. It was administered under the direction of the Materials Directorate, Wright Laboratory, Air Force Materiel Command, Wright-Patterson Air Force Base, Ohio, with Dr. W. W. Adams as the project scientist. Co-authors were Jennifer A. Young and Dr. Barry L. Farmer of the University of Virginia, and Dr. W. Wade Adams of the Materials Directorate. The report covers research conducted from 1 September 1992 to 15 August 1994.

The authors (J. A. Young and B. L. Farmer) wish to acknowledge partial financial support from Virginia Center for Innovative Technology and Imaging Science Technologies Inc., Charlottesville, VA.

## ABSTRACT

Photochromic materials are of interest to the Air Force for a variety of potential applications including high resolution photography, optical devices, holographic systems and variable transmission devices.

The photochemical and structural characteristics of two organic photochromes, specifically indoline-spiro-benzopyran and benzothiazoline-spiro-benzopyran, have been studied by computational chemistry techniques. Both quantum mechanical and classical methods were used. Irradiation of spiropyran by UV light causes molecular rearrangement, thus yielding merocyanine whose absorption band lies in the visible region. This is the basis of the photochromic nature of the spiropyran. Several chromophore based devices would benefit from a material whose visible absorption spectrum was red shifted and whose structure and properties in various environments was fully understood.

The absorption spectra of both indoline-spiro-benzopyran and benzothiazoline-spiro-benzopyran were calculated. Spectroscopic calculations reveal that the absorption spectrum is determined by two factors: the choice of substituent and the geometry of the chromophore. Both electron withdrawing and electron donating substituents were strategically placed on the chromophore. Maximum red shifts may be achieved in the merocyanine by attaching (at the proper position) strongly electron donating substituents which force rotations about double bonds while limiting the rotation about single bonds.

Two force fields have been developed to allow classical calculations on large photochromic systems (solvated chromophores or polymer substituted chromophores). The agreement of these classical force fields with quantum mechanical methods for the unsubstituted indoline-benzopyran merocyanine has been shown. These force fields were used in molecular dynamics simulations to explore the effect of the solvent polarity on the chromophore. The calculations demonstrated the ability of polar solvents to stabilize the merocyanine form, thus potentially reducing the fading rate of the chromophore.

## Section I

# INTRODUCTION

### 1.1 Motivation

Photochromic compounds have attracted considerable attention in the past two decades. Along with pure scientific intrigue, considerable commercial interest has been expressed in the photochromic phenomenon. Specifically, the photochromic properties of spiropyrans, which were first noted by Fischer and Hirshberg in 1952, have led to intensive research into the fundamentals and the applications of spiropyran.<sup>1</sup> Yet many questions remain unanswered. The structure of the chromophore may easily be altered, thus yielding various chromophores with differing characteristics. Practical applications require that the spiropyran be placed in a host matrix. Host matrices such as crystalline or amorphous forms of a compound, solvents or polymers may be used over a wide range of temperatures, viscosities, pressures and electric or magnetic field strengths.<sup>2</sup> Investigating the influence that these factors have on spiropyran will aid in the development of new devices. Current applications include high resolution photography, optical devices, variable transmission devices, photovoltaic and holographic systems.<sup>3</sup>

## 1.2 Photochromism

When irradiation by light causes a change in the color of a material that material is said to be photochromic. Spiropyrans are a class of organic photochromes which have been well documented. The change in color upon irradiation is the result of increased conjugation due to the molecular rearrangement scheme shown in figure 1.1. Originally in the closed form, the heterocyclic (H) and pyran fragments are linked by a tetrahedral  $sp^3$  hybridized carbon atom. The  $\pi$  electron systems are orthogonal and therefore non-interacting. The primary absorption bands of the spiropyran lie in the ultraviolet region of the electromagnetic spectrum.

Irradiation of the spiropyran with ultraviolet light transforms it into its open, merocyanine form. Photodissociation of the C-O  $\sigma$  bond occurs via the  $\alpha$ -mechanism in which the C-O  $\sigma$  bond is weakened due to its overlap with the vacant n orbital of the nitrogen.<sup>4</sup> This process is followed by molecular rearrangement in which the heterocyclic and pyran portions of the molecule become coplanar and the central carbon atom becomes  $sp^2$  hybridized. These changes allow the delocalization of the  $\pi$  electrons between the two fragments. Numerous isomers are possible.<sup>5</sup> Shown in figure 1.1 are the two electronic extremes of the most stable mesomeric forms, the dipolar zwitterion with localized charges and the apolar quinonic form. Analysis of the charge distributions shows that electronically, the merocyanine is a hybrid of these two isomers. The absorption band of the chromophore is shifted into the visible region of the electromagnetic spectrum and as a result the material acquires a blue color.

The closed/open process is reversible by heat or light absorption in the absorption band of the merocyanine. However, photochromes generally lose their ability to change colors after repeated closed-open transitions. This process, known as fatigue, must be

considered in practical applications for it occurs after anywhere from 5 to 30,000 transitions, depending upon the specific chromophore.<sup>6</sup>

Many photochromic spiropyrans have been synthesized and studied in the past.<sup>7</sup> The basic chemical structure of the spiropyran class of organic chromophore is seen in figure 1.1. The spiropyran is classified (named) by specifying the heterocyclic portion (H), the pyran portion and any substituents (R'). The base molecules which are of particular interest are the indoline-spiro-benzopyran (BIPS) and the benzothiazoline-spiro-benzopyran. Three initial substitutions have been made to both spiropyran compounds. The methyl group on the nitrogen was replaced by an isopropyl group. A nitrate group and a methoxy group were placed at positions 6 and 8, respectively, on the pyran ring. These substitutions increase the probability of C-O bond cleavage and the stabilization of the merocyanine form.<sup>8</sup> The official names of these molecules are the 1'-isopropyl, 3',3'-dimethyl-indoline-spiro-6-nitro-8-methoxy-benzopyran and 1'-isopropyl-benzothiazoline-spiro-6-nitro-8-methoxy-benzopyran. For simplicity, these molecules will be referred to as the unsubstituted indoline-spiro-benzopyran and benzothiazoline-spiro-benzopyran, respectively (figures 1.2 and 1.3). Various substituents will later be placed upon these chromophores.

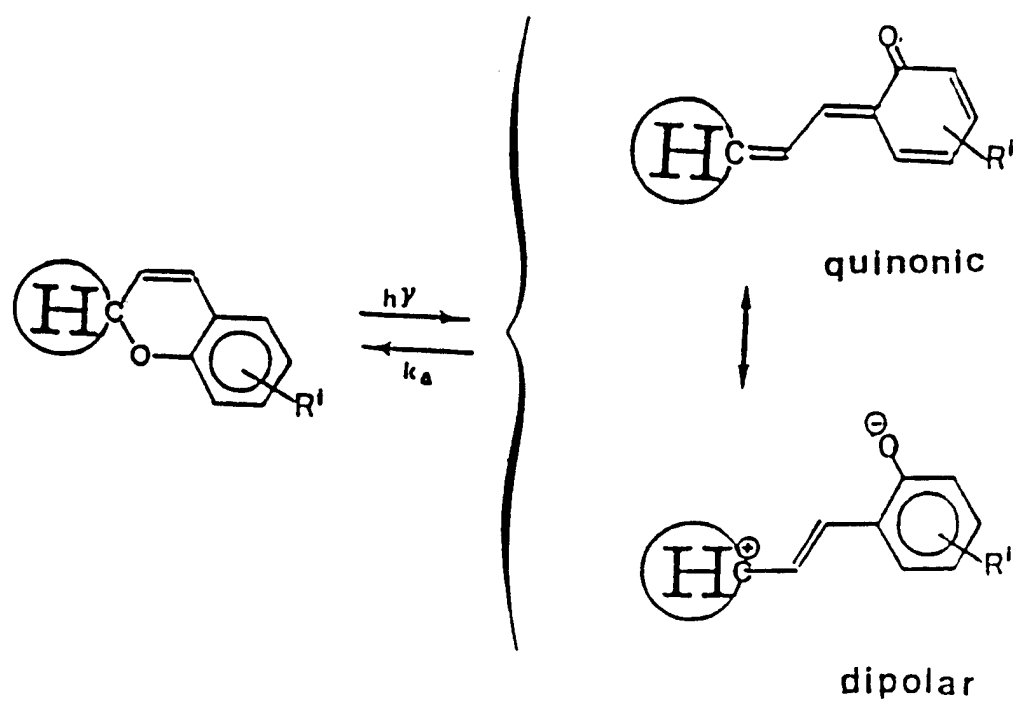


Figure 1.1: Photochromism of spiropyran yields the apolar quinonic form and dipolar zwitterion form, respectively.

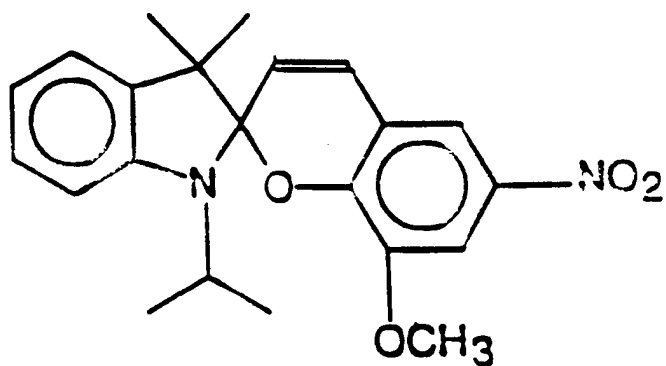


Figure 1.2: The indoline-spiro-benzopyran.

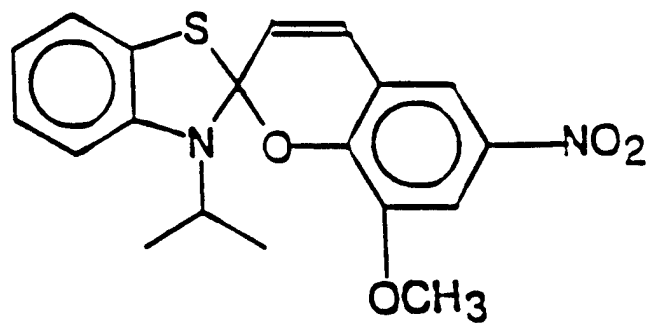


Figure 1.3: The benzothiazoline-spiro-benzopyran.



### 1.3 Factors Influencing Photochromism

The photochromism of spiropyran is strongly dependent upon two main variables: the specific structure of the spiropyran itself and its host matrix. The structure of the molecule (the hetero atoms and substituents) defines the stereo-electronic parameters of the system. These parameters have steric and direct electronic effects, both inductive (by way of sigma bonds) and mesomeric (by way of  $\pi$  bonds and nonbonded interactions).<sup>9</sup> The stereo-electronic parameters such as substituents influence the rate at which the merocyanine reverts to the spiropyran (i.e., the fading rate) and the wavelength at which the system exhibits maximum absorption.

The choice of matrix within which the photochromic molecules is placed is also important. The density of the matrix helps determine both the spectral kinetic and the thermodynamic properties of the system.<sup>10</sup> Spiropyrans exhibit photochromism in solvents of a wide range of polarities (water to hexane). The polarity and its macroscopic counterpart, the dielectric constant, will alter the electronic interactions of the system. In general, polar solvents tend to stabilize charge separation in the merocyanine form, thus stabilizing this form.<sup>11</sup> For example, the fading rate is  $10^2$  slower in ethanol than in toluene for the indoline-spiro-benzopyran chromophore ( $0.6 \text{ sec}^{-1}$  vs  $6 \times 10^{-3} \text{ sec}^{-1}$ ).<sup>12</sup> Solvatochromic effects are seen as the polar solvent generally shifts the visible absorption to shorter wavelengths.<sup>13</sup> Both liquid crystalline environments and Langmuir Blodgett films show exciting prospects for embedding chromophores to be used in optical devices.

## 1.4 Technological Applications

The utilization of photochromic materials has lead to the invention of many practical devices along with the improvement of established devices. Both the photosensitivity and the reversibility of the material are exploited for commercial needs. Applications such as self-developing photography and protective wrappers for photosensitive products make use of the photosensitivity of the photochrome.<sup>14</sup> Photochromes also offer the unique ability to revert to their original state and thus lend themselves to reusability. Chemical switches for computers, data displays, optical signal processing and reusable information storage media take advantage of this property.<sup>15</sup> This research, done in conjunction with Imaging Science Technologies (IST), Virginia Center for Innovative Technology (VCIT) and the Hardened Materials Branch at Wright-Patterson Air Force Base, seeks to contribute to the utilization of photochromic materials in the development of advanced imaging techniques. Organic chromophores are utilized in IR imaging devices and programmable polarizing elements.

The ability to convert infrared images into visible images via an all-optical process would be a significant scientific breakthrough. Such a device would lower the cost of traditional infrared-visual converters (i.e., night vision devices). An all-optical process would eliminate the need for electronic scanning and processing along with the cooling requirements of current technologies. Night vision could become a fast response, inexpensive technology. The physics of creating an infrared image by means of optical activity is detailed elsewhere.<sup>16</sup> One proposed mechanism has as its basis the theory of coupled oscillators (W. Kuhn, 1930). The idea is to couple oscillators (dipoles) sensitive to the visible and infrared frequencies of the electromagnetic spectra. Crosslinking an IR sensitive polymer to a chromophore, permanently secured in its merocyanine form, might be one way of achieving this objective. The merocyanine is ideal for such an application

because of its high optical activity. The ability to tailor the optical properties of the merocyanine will be explored in this thesis.

Taking advantage of the high rate of the reversible photochemical process of the spiropyran has also led to the concept of Optically Programmed Polarizing Elements (OPPE). Here the spiropyran acts as a switch connecting conducting polymers which have selected absorption bands (polydiacetylene, polythiophene etc.). The system would be nonconducting when the chromophore is in the spiropyran form and conducting when the merocyanine form is present. Due to the differences in the extent of conjugation of the two systems, different absorption bands would accompany the change in conductivity. Extended conjugation gives long wavelength absorption bands while limited conjugation yields short wavelength absorptions. Preferential orientation of the polymer-chromophore backbone would allow the material to form a conducting network upon illumination. This material would then function as a polarizing element. The ability to predict the structural changes of the chromophore as a function of time, temperature and environment will be explored in this thesis.

## 1.5 Approach

Organic photochromic systems may be engineered to fulfill a wide variety of purposes. This is possible due to the large number of parameters which may be varied. The techniques of computational chemistry have been employed to guide the development of photochromic systems having the desired structural and optical characteristics. The SYBYL molecular modeling software (distributed by TRIPOS Associates Incorporated) is the primary tool used for these computations. This software package contains procedures to calculate classical molecular geometries and the dynamics of the molecular system. MOPAC, a semiempirical molecular orbital package, allows quantum mechanical

calculations of the molecular geometries and heats of formation to be done. Finally, the spectroscopic properties of the molecules are investigated using the quantum mechanical program ZINDO. All of the aforementioned programs are run on an IBM RS/6000 Model 340 workstation equipped with graphics capabilities.

The goal of this research is to obtain a better understanding of the spiropyran photochromic system. Extensive interest has been expressed in the indoline-spiro-benzopyran and benzothiazoline-spiro-benzopyran shown in figures 1.2 and 1.3 respectively. Characterization of the molecular geometries and the resulting charge distributions is important in understanding the spectral and kinetic properties of the system. Means of shifting the merocyanine absorption band to longer wavelengths is important in the development of the optical devices under consideration. Modeling seeks to identify chromophores and substituents (along with their placement) which aid this purpose. Further, the interactions between the chromophore and its matrix will be studied. Issues such as the optical properties of the photochromic system and the stability of the merocyanine will be addressed.

## Section II

### THEORY

Computational chemistry computer modeling is an efficient means of investigating molecular systems. Structure and property calculations at the atomic level can be applied to phenomenological models which in turn may be used to describe macroscopic features. Three methods of computational modeling on the molecular level are common: *ab initio* calculations, semiempirical calculations and force field calculations. Limitations in the number of atoms that can be examined by *ab initio* methods preclude their use for the spiropyran. Thus the later two methods are of most use in probing the photochromic spiropyran system. These are discussed in detail below.

#### 2.1 Quantum Mechanics

Since the development of molecular orbital techniques in 1951 by Roothaan and Hall, these techniques have been used to probe chemical reactions, bond orders, charge distributions, polarizabilities and spectroscopic aspects of molecular systems.<sup>17</sup> Unfortunately, the size of the system which may be studied using these techniques is limited to several tens of atoms.

### 2.1.1 LCAO/SCF Method

Quantum mechanics can provide an understanding of the relation between the electronic spectrum and the molecular structure of the chromophore. Schrodinger's equation uses wave functions to describe systems consisting of nuclei and electrons. The Born-Oppenheimer approximation allows one to examine the electronic time-independent differential Schrodinger's equation:

$$\mathbf{H}_e \psi = E \psi \quad (2.1)$$

$\psi$  is the electronic wave function and  $E$  is the energy.  $\mathbf{H}_e$  is the electronic Hamiltonian which consist of two terms.

$$\mathbf{H}_e = \sum_i \mathbf{h}_i + \sum_{i,j} \mathbf{V}_{i,j} \quad (2.2)$$

The one electron operator (the first term) accounts for the kinetic energy and the nuclear attraction of single electrons. The second term of the Hamiltonian describes interelectron repulsion.<sup>18</sup> Electron motions are very rapid in comparison to the vibrational motions of the nuclei. Thus, electronic transitions do not cause an instantaneous change in the nuclear configuration of the molecule (the Franck-Condon principle). This principle allows the vibronic interactions to be ignored.<sup>19</sup> Even so, exact solutions of Schrodinger's equation can only be found for single electron-single nucleus systems. This is due to the complexity of the mathematics which arises from terms containing coordinates of two particles as variables. Approximations are therefore made when investigating the many electron systems which are of interest.

The single-determinant electronic wavefunction,  $\psi$ , for a closed shell molecule containing  $n$  electrons is the Slater determinant of spin orbitals,  $S_n(n)$ .

$$\psi = \det [ S_1(1) \dots S_n(n) ] \quad (2.3)$$

Molecular orbitals are assumed to be linear combinations of the atomic orbitals of the molecule.

$$S_n = \sum_u C_{nu} B_u \quad (2.4)$$

where  $B_u$  is an atomic orbital,  $C_{nu}$  is the expansion coefficient, and  $S_n$  is the molecular orbital (MO). This is the Linear Combination of Atomic Orbitals (LCAO) MO method. If a complete basis  $\{B_u\}$  is used, no errors arise, but such computations are very demanding. Instead approximations are made by restricting the set of atomic orbitals to be used. The application of variational theory to the energy computed by the LCAO MO method gives the Self-Consistent Field (SCF) secular equation.<sup>20</sup>

$$| \mathbf{H}^f - \epsilon \mathbf{S} | = 0, \quad (2.5)$$

where  $\mathbf{H}^f$  is the Fock operator, an effective one electron Hamiltonian in matrix form.  $\epsilon$  is the one electron energy eigenvalue and  $\mathbf{S}$  is the orthonormal overlap matrix of  $S_n$  orbitals. The equation is solved self consistently. In the solution of this equation we find the properties of a pseudo particle in an average field defined by all other particles.<sup>21</sup> This method, the LCAO/SCF method, determines optimal molecular orbitals within the limits of the finite basis approximation.

Evaluating the numerous integrals which evolve during the calculations may be done in one of two ways. *Ab initio* methods calculate the integrals explicitly and are thus known as first principles methods. On the other hand, semiempirical MO methods provide efficient approximations by parameterizing the integrals. Values of the integrals are chosen to reproduce a range of selected molecular properties (heats of formation,

molecular geometries and molecular absorption spectra) and to give minimal uniform errors in the geometry and spectra over a selected set of compounds.<sup>22</sup>

Modeling the interelectronic interactions,  $\sum_{i,j} V_{i,j}$  of the electronic Hamiltonian, is necessary to calculate molecular properties accurately. Two major model Hamiltonians are used, Complete Neglect of Differential Overlap (CNDO) and Intermediate Neglect of Differential Overlap (INDO). CNDO omits the one-center two-electron exchange integrals which means that different spin multiplets can not be distinguished. Different spin multiplets may be discerned by the inclusion of the two-electron exchange integrals via INDO (i.e., singlet and triplet transitions are nondegenerate).<sup>23</sup> The parameter sets which best describe the thermodynamic and geometric aspects of a molecule are MINDO (Modified Intermediate Neglect of Differential Overlap), MINDO/3, PM3 (Parametric Method) or AM1 (Austin Model).<sup>24</sup> In this research, MOPAC, a quantum mechanics program, along with the AM1 parameterization is used to calculate the geometry of a molecule. ZINDO, another semiempirical molecular orbital computational chemistry program, is used with the INDO1 (Intermediate Neglect of Differential Overlap) parameters to calculate the spectroscopic properties of a molecule.

### 2.1.2 Configuration Interaction

Configuration interaction (CI) accounts for the mutual repulsion of the electrons which leads to interactions between the various excited configurations. This greatly improves the quality of spectroscopic data. When  $n$  basis functions are used in the one electron approximation LCAO/SCF method, a finite number of occupied orbitals ( $o$ ) and unoccupied ( $v$ ) orbitals result where  $n=o+v$ . Singly excited state spin configurations, ( $\Delta_i$ ), are produced by promoting an electron from an occupied orbital to an unoccupied orbital. The spectroscopic (CI) wave function ( $\Psi^{CI}$ ) is the linear combination of such determinants.



$$\Psi_{CI} = \sum c_i \Delta_i \quad (2.6)$$

Application of the variational principle yields the eigenvalue problem:

$$| \mathbf{H}_e - E \mathbf{S} | = 0. \quad (2.7)$$

This gives the energy (eigenvalue) and the coefficients corresponding to the CI wavefunction. The  $\mathbf{H}_e$  and  $\mathbf{S}$  matrices now involve the n-electron determinants. Physically, the excited (antibonding) orbitals which were unoccupied in the LCAO/SCF approximation are partially filled after CI mixing. Likewise some of the electronic occupation of the ground state (bonding) LCAO/SCF orbitals has decreased in the CI ground state orbitals.<sup>25</sup>

LCAO/SCF calculations (via MOPAC) were done to obtain an accurate ground state molecular geometry. CI calculations (via ZINDO) were then done to acquire the electronic spectra (the transition energies and corresponding oscillator strengths of the molecule). This is the manner in which the electronic spectrum of a molecule was obtained. The possible frequencies (wavelengths) of absorptions are simply the energy differences that arise when exciting an electron from CI orbital m to orbital n ( $E_n - E_m = h\nu_{mn}$ ). The strength (probability) of a given transition is denoted by a unitless quantity called the oscillator strength ( $f_{mn}$ ).<sup>26</sup>

$$f_{mn} \equiv 1.085 \times 10^{-5} \nu_{mn} \mathbf{M}_{mn}^2 \quad (2.8)$$

$\nu_{mn}$  is the wavenumber of the transition ( $\text{cm}^{-1}$ ).  $\mathbf{M}_{mn}$  is the electronic transition moment of the transition between states m and n (M has units of  $\text{\AA}$ ), given by

$$\mathbf{M}_{mn} = \langle \Psi_n | \mu | \Psi_m \rangle \quad (2.9)$$

where  $\mu$  is the electric dipole moment operator for the molecule. The transition moment is seen to depend on the nature of the initial and final electronic spatial wavefunctions. Oscillator strengths of  $\approx 1.0$  indicate a strong transition. A Lorentzian line-shape can be used to approximate an absorption band.<sup>27</sup> Thus, superimposing Lorentzian curves (centered at the appropriate energies and having magnitudes proportional to the oscillator strengths) for each electronic transition will give a spectrum which can be compared with experimental spectra.

MOPAC and ZINDO have inherent but different strengths and weaknesses and are generally used for distinct purposes. The parameters of MOPAC are best suited to determine molecular geometries, heats of formation and charge distributions, while those of ZINDO are optimized to reproduce spectral data. By combining these methods, this research exploits the strengths of the respective programs while minimizing their inherent weaknesses.

## 2.2 Classical Mechanics

Force field methods often are invoked to answer questions concerning molecular conformations, molecular interactions in various environments and for performing simulated annealing as a means of locating energy minima. The method is advantageous in that it allows one to study the structures and dynamics of large systems (hundreds of atoms). The disadvantages (though they are not insurmountable) are that one is unable to examine changes in electron distribution or changes in bonding (i.e., chemical reactions). Accurate results can be obtained only when the force field parameters correctly describe the specific system in question.

Force field calculations are based on a classical (as opposed to quantum mechanical) description of a molecule. The molecule is viewed as a collection of masses (atoms) and springs (bonds). Molecular conformations are investigated by minimizing a classical potential energy function, PE. It is important to note that PE is only a measure of the intramolecular strain relative to a hypothetical (parameterized) system having geometric features which are independently optimizable. The potential energy function is the sum of contributions arising from bond stretching, angle bending, out of plane bending, torsional rotation and non-bonded interactions. Optionally, electrostatic contributions and distance, angle or torsional constraints may also be considered.

$$PE = \sum E_{\text{stretch}} + \sum E_{\text{bend}} + \sum E_{\text{out of plane}} + \sum E_{\text{torsion}} + \sum E_{\text{van der Waals}} + [\sum E_{\text{electrostatic}} + \sum E_{\text{constraints}}] \quad (2.7)$$

The specific form of the energy term associated with bond stretching and compression is given by:

$$E_{i,j} = k_{i,j} * (d_{i,j} - d_{i,j}^0)^2 \quad (2.8)$$

$k_{i,j}$  is the bond stretching force constant (kcal/mol Å<sup>2</sup>),  $d_{i,j}$  is the actual bond length (Å), and  $d_{i,j}^0$  is the optimal bond length (Å). The angle bending energy term is:

$$E_{i,j,k} = k_{i,j,k} * (\theta_{i,j,k}^0 - \theta_{i,j,k})^2 \quad (2.9)$$

$k_{i,j,k}$  is the angle bending force constant (kcal/mol degree<sup>2</sup>),  $\theta_{i,j,k}^0$  is the optimal angle (degrees) and  $\theta_{i,j,k}$  is the actual angle (degrees). The TRIPOS torsional potential energy function between four bonded atoms, i, j, k and l is:

$$E = k_{i,j,k,l} (1 + (s/|s|) \cos(|s| \phi_{i,j,k,l})) \quad (2.10)$$

where  $k_{i,j,k,l}$  is a parameter which describes the torsional barrier (kcal/mol-degree<sup>2</sup>),  $s$  is the periodicity of the function and  $\phi_{i,j,k,l}$  is the torsion angle (degrees).

The parameters which define these potential functions are found by fitting experimental properties such as geometries, conformational energies, heats of formation, or crystallographic data. Numerous force fields (collections of parameters and energy expressions) have been developed to provide information concerning the properties of various molecular systems. Some examples are MM2, which is used for small molecules, Amber and CHARMM, which are used for biopolymers, and TRIPOS which is designed for use on a wide variety of organic molecules.<sup>28</sup>

### 2.2.1 Molecular Mechanics

Once a proper force field has been identified or obtained, molecular mechanics (MM) calculations may be used to predict molecular geometries. This is accomplished by minimizing the potential energy with respect to the atomic coordinates. Of the many minimization techniques available, the iterative steepest descent method is most often used. Major distortions and bad steric interactions are removed easily as the program searches for an energy minimum. The Powell method uses more advanced rules than the steepest descent method to determine an energy minimum. The energy minimum found, however, may be a local minimum rather than a global minimum.

### 2.2.2 Molecular Dynamics

Molecular dynamics (MD) calculations allow the study of the time averaged motion of a molecular system. The molecular system is defined in terms of the initial Cartesian coordinates of the atoms and a specified force field. An initial velocity is applied to each of the atoms and Newton's equation of motion ( $\mathbf{F} = m \mathbf{a}$ ) is integrated to yield the

trajectories of each atom. This is an iterative process over many time steps, usually  $\Delta t = 1$  fs. Constant temperature or pressure simulations are carried out for various lengths of time.

Solvent-solute interactions are studied through molecular mechanics and molecular dynamics. Solute molecules can be placed in various solvent environments. MD calculations used to equilibrate and then to simulate the solvent-solute system at a given temperature. The resulting solvent-solute interactions may then be analyzed. This is an important aspect of the computer modeling in that it allows the examination of molecular structure and behavior within various environments as opposed to in vacuum.

## Section III

### RESULTS AND DISCUSSION

Calculations have been made to provide a better understanding of both the photochemical and the structural characteristics of the indoline-spiro-benzopyran and the benzothiazoline-spiro-benzopyran systems shown in figures 1.2 and 1.3 respectively. Both the spiropyran and merocyanine forms have been investigated. Spectroscopic calculations and detailed modeling of the merocyanine form in various solvent environments has been done.

#### 3.1 Spectroscopic Modeling

The ability to accurately calculate the electronic absorption spectra of photochromic molecules is of great importance. Knowledge of the absorption spectra as a function of molecular geometry, choice and placement of substituents, and molecular environment is vital in the development of optical devices. The electronic spectral peaks are sharpest in vacuum where the solvent-solute interactions (solvatochromic effects) which lead to peak broadening, are absent.<sup>29</sup> The following calculations were thus done in vacuum. Understanding the effects that molecular geometry, substituents and the environment have on the spectra will allow the optimal optical properties to be obtained.

### 3.1.1 Methodology

Obtaining an accurate ground state molecular geometry of the molecule is first necessary. The spiropyran and merocyanine molecules were initially built through the SYBYL interface. When considering the merocyanine, the dipolar form was used as the starting geometry. The choice of this particular starting point will not impact the results since the molecular mechanics bond types with which the molecule was built are irrelevant in molecular orbital calculations. MOPAC with the AM1 parameterization was then used to minimize the molecular energy, thus optimizing the geometry. Several initial geometries were surveyed to assure the location of the global energy minimum.

ZINDO was then employed to calculate the spectroscopic features of these optimized molecules. The INDO1 Hamiltonian was chosen to represent interelectronic interactions.<sup>30</sup> Configuration Interaction (CI) calculations were performed to obtain the spectroscopic transition energies and corresponding oscillator strengths. The oscillator strengths are sensitive to the number of excitations in the CI calculation. Due to the large energy difference required to excite a core electron (approximately 1000 eV) and an outer electron (approximately 10 eV), only the outermost electrons (the optical electrons) are included in the CI calculation.

The electronic spectrum of a spiropyran has been calculated previously using the CNDO extended Hamiltonian along with CI.<sup>31</sup> The CI was done by "considering the 30 lowest excited singlet and triplet monoexcited configurations". The present research uses this same number of monoexcited configurations and the more thorough INDO1 extended Hamiltonian. Test molecules and agreement with earlier CNDO work were used to validate this method. Figure 3.1 shows the experimental spectrum and the major calculated transitions of naphthalene. Since the agreement between the experimental and the calculated spectrum is good, this method was then applied to the specific chromophores of interest.

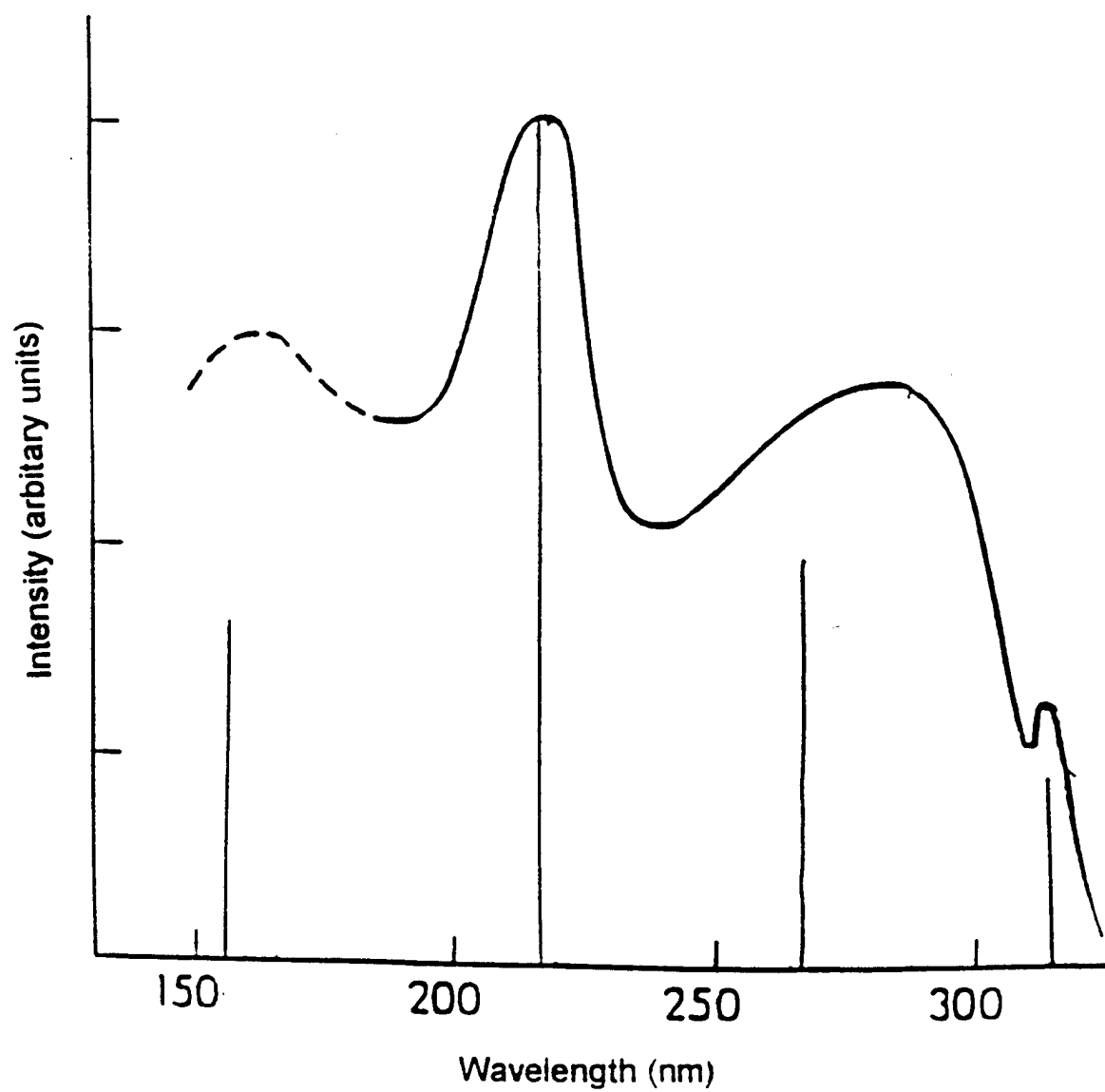


Figure 3.1: The experimental (curve) and calculated (spikes) spectra of naphthalene.

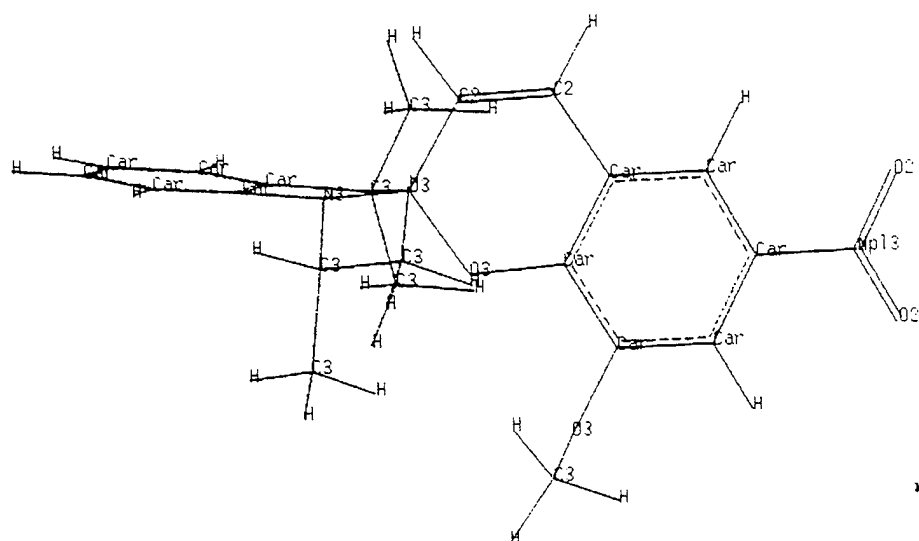


### 3.1.2 The Indoline-spiro-Benzopyran

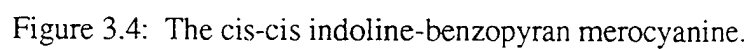
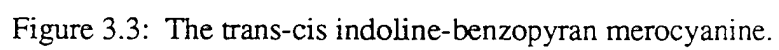
The chromophore upon which this research will focus is the indoline-spiro-benzopyran. The optimized geometry of the indoline-spiro-benzopyran shows that the constituent rings of the spiropyran occupy two planes as expected (figure 3.2). The unsubstituted indoline-benzopyran merocyanine has four stable isomers which differ by  $180^\circ$  rotations about the first and third central bonds which link the indoline and benzopyran fragments of the merocyanine. The isomers are characterized by the dihedral angles of the three central carbon bonds, bonds 1, 2 and 3 in figure 2.  $\phi_1$  is defined by atoms 3', 2', 2 and 3.  $\phi_2$  is defined by atoms 2', 2, 3, and 4. While  $\phi_3$  is defined by atoms 2, 3, 4, and 5. The trans-cis, cis-cis, trans-trans and cis-trans isomers are shown in figures 3.3-3.6, respectively. Figure 3.7 demonstrates the planarity of the rings in the merocyanine. The computed heats of formation (AM1 parameterization) of these isomers differ by less than 2 kcal/mol as seen in table 3.1. The relative stability of the four isomers is trans-cis > cis-cis > trans-trans > cis-trans. This ordering is sensitive to the substituents on the rings. Previous results have shown that when the 8-methoxy is removed and the 1' isopropyl is replaced by methyl, a different ordering arises (trans-cis > trans-trans > cis-cis > cis-trans).<sup>32</sup> This can be attributed to the difference in nonbonded interactions which arise in these two systems.

| Indoline-benzopyran     | Heat of Formation (kcal/mol) |
|-------------------------|------------------------------|
| spiropyran              | 18.58                        |
| trans-cis merocyanine   | 20.06                        |
| cis-cis merocyanine     | 20.77                        |
| trans-trans merocyanine | 21.14                        |
| cis-trans merocyanine   | 21.80                        |

Table 3.1: Calculated heats of formation of the indoline-benzopyran.



23



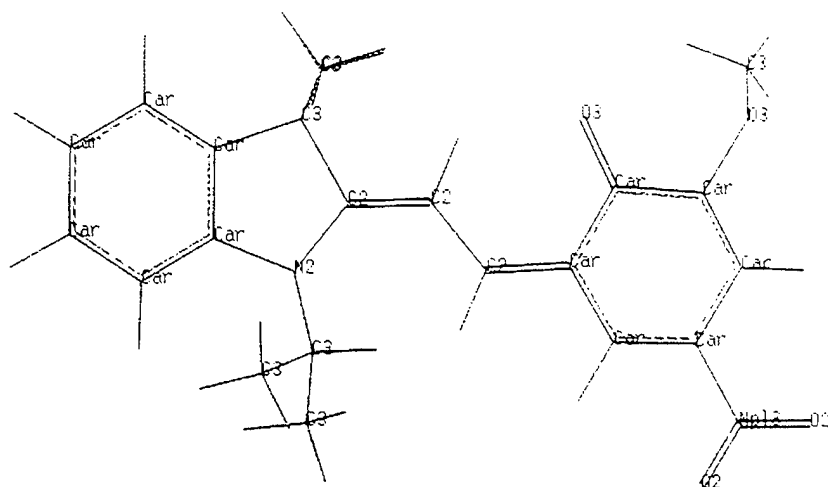


Figure 3.5: The trans-trans indoline-benzopyran merocyanine.

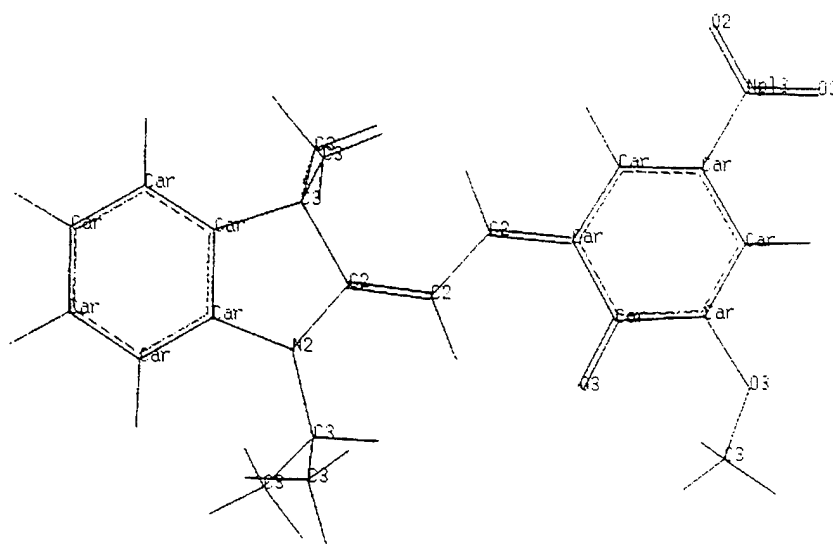


Figure 3.6: The cis-trans indoline-benzopyran merocyanine.



shown absorption peaks around 340 nm, as well as peaks around 255 nm which are two to five times more intense (figure 3.8).<sup>34</sup> C-O bond cleavage under the influence of UV light with  $\lambda < 300$  nm is due to the transfer of the electronic excitation energy from the indoline to the benzopyran portion of the molecule.<sup>35</sup> This is easily understood by noting that a 270 nm (4.59 eV) absorption supplies enough energy to break the carbon-oxygen single bond (3.71 eV). The experimental spectrum shows the two aforementioned peaks to lie at 255 nm (4.86 eV) and 340 nm (3.65 eV). The calculated spectrum, figure 3.9, places them at 270 nm (4.59 eV) and 345 nm (3.59 eV) in excellent agreement with the experimental spectrum.

The CI data show that the electronic transition from the ground state highest occupied molecular orbital (HOMO, g) to the lowest unoccupied CI orbital (LUMO, 1),  $g \rightarrow 1$ , is not a dominant transition in the unsubstituted indoline-spiro-benzopyran. Instead, the transition from the HOMO to the fifth unoccupied orbital,  $g \rightarrow 5$  at 270 nm, is responsible for the C-O bond cleavage.  $\Psi^2$  for the HOMO (g), LUMO (1) and fifth unoccupied (5) orbitals are shown in figures 3.10, 3.11 and 3.12 respectively. The HOMO and the LUMO reside on opposite halves of the chromophore. The wavefunction,  $\Psi$ , has both spatial and spin components. Thus, due to the spatial dependence of the transition moment (equation 2.9), the  $g \rightarrow 1$  transition has a low oscillator strength. Spiroyrans having a nitro group demonstrate low-energy  $\pi-\pi^*$  transitions which involve intramolecular charge transfer.<sup>36</sup> Orbital 5 is located directly above the HOMO, thus allowing the intramolecular charge transfer transition from the indoline fragment to the benzopyran fragment of the spiropyran. This explains the high oscillator strength of the  $g \rightarrow 5$  transition.

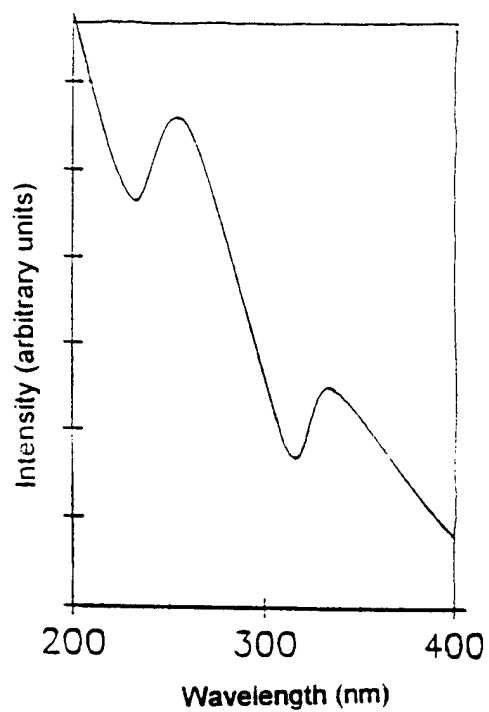


Figure 3.8: The experimental spectrum of the indoline-spiro-benzopyran.

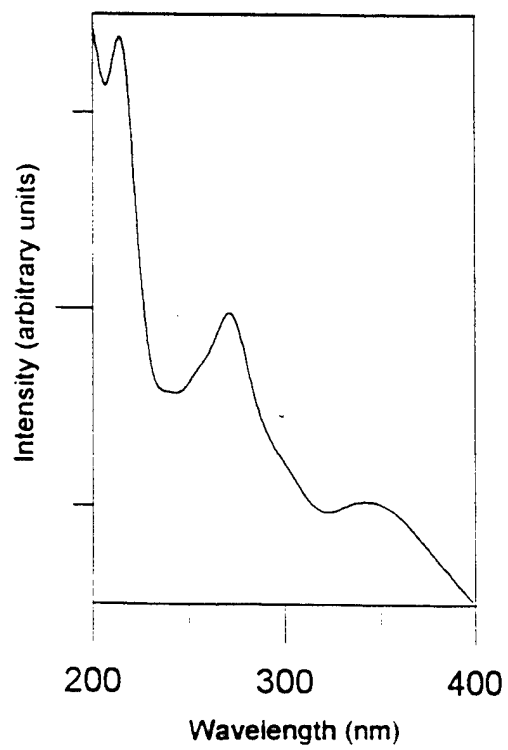


Figure 3.9: The calculated spectrum of the indoline-spiro-benzopyran.

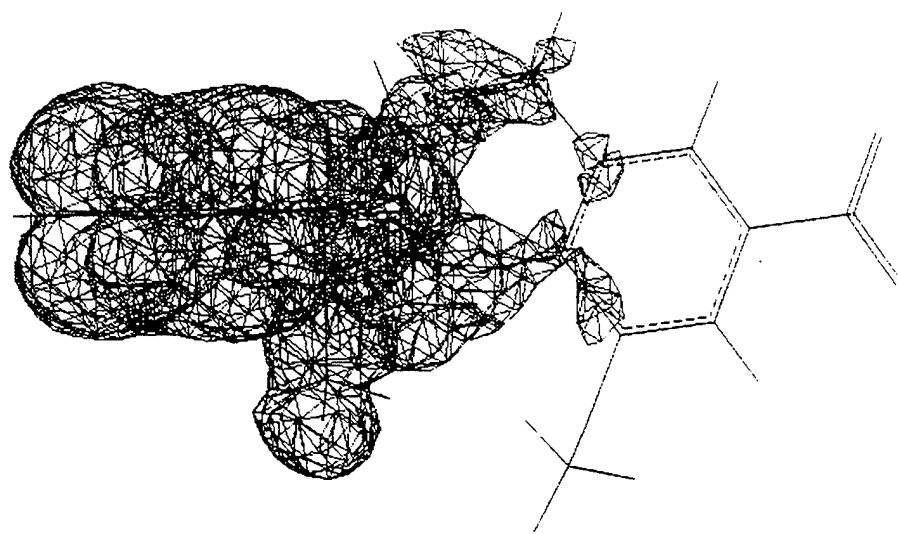


Figure 3.10: The HOMO (g) of the indoline-spiro-benzopyran.

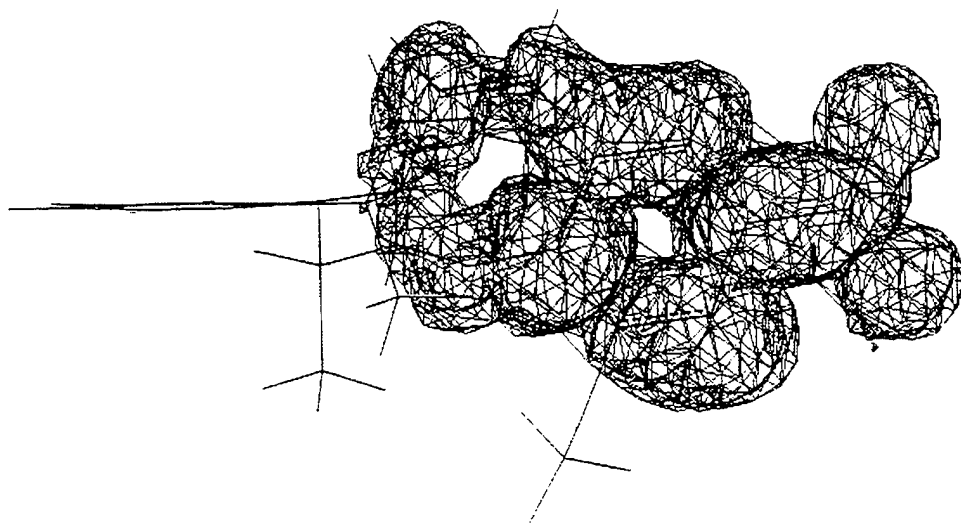


Figure 3.11: The LUMO (1) of the indoline-spiro-benzopyran.



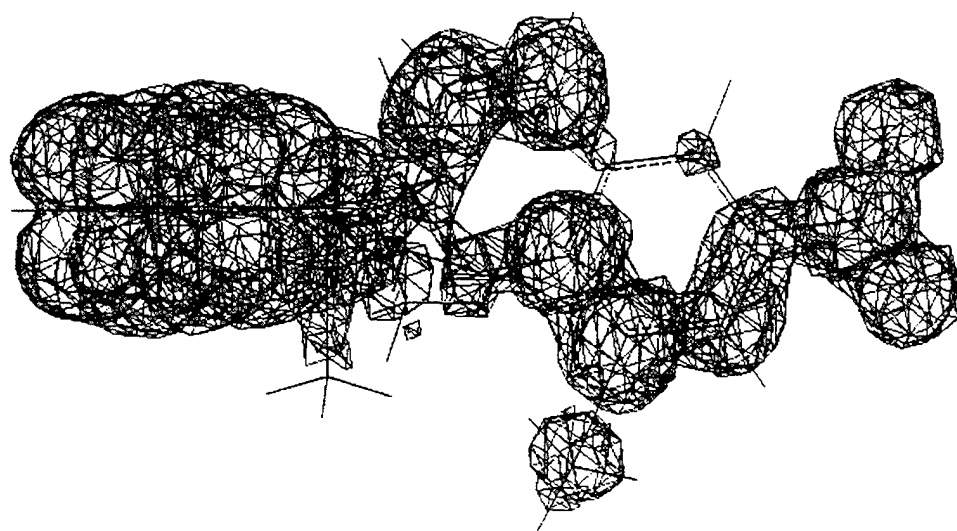


Figure 3.12: The fifth unoccupied orbital (5) of the indoline-spiro-benzopyran.

The absorption spectrum of the unsubstituted indoline-benzopyran merocyanine is now examined. The trans-cis indoline-benzopyran merocyanine, the lowest energy isomer in table 3.1, was first examined. Compared to the spiropyran, the absorption peak of the merocyanine is shifted into the visible region as a result of the increased  $\pi$  delocalization that occurs in the planar form. Figures 3.13 and 3.14 show the experimental and calculated spectra of the merocyanine. The  $g \rightarrow 1$  transition which occurs at 461 nm is now the dominant transition. The delocalization of both HOMO and LUMO, figures 3.15 and 3.16, explains the high probability with which the electrons move between these orbitals.

It is important to note that the quantum mechanical procedures used yield only semi-quantitative information about the absorption spectra. Therefore, the relative positions of the peaks are more significant than their absolute positions.

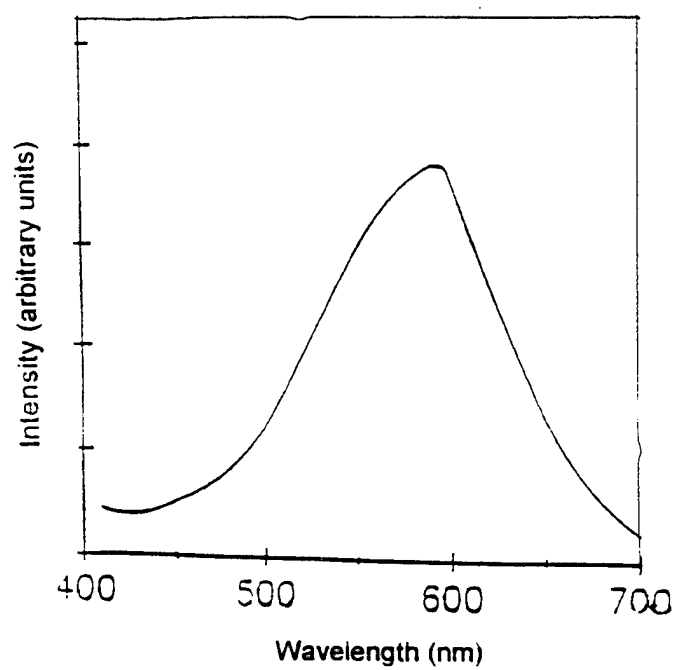


Figure 3.13: The experimental spectrum of the indoline-benzopyran merocyanine.

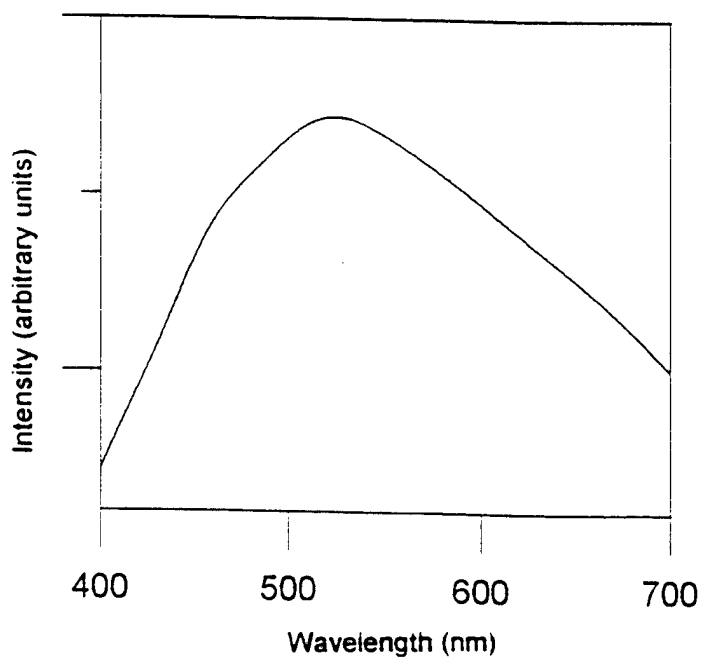


Figure 3.14: The calculated spectrum of the indoline-benzopyran merocyanine.

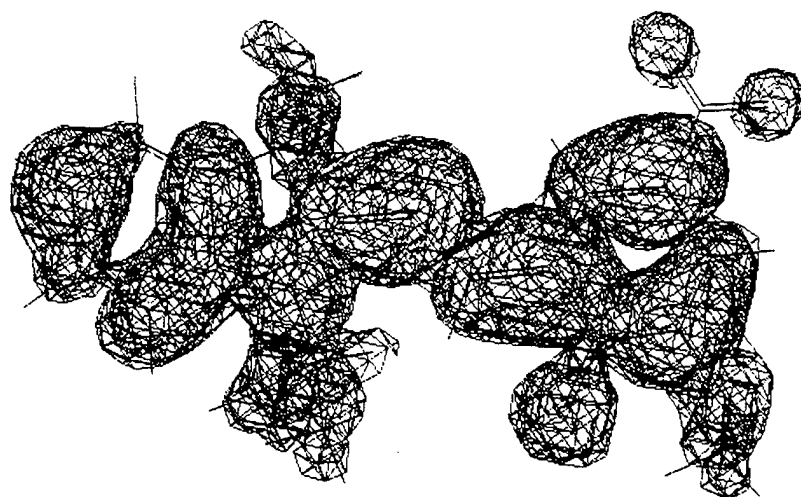


Figure 3.15: The HOMO of the indoline-benzopyran merocyanine.

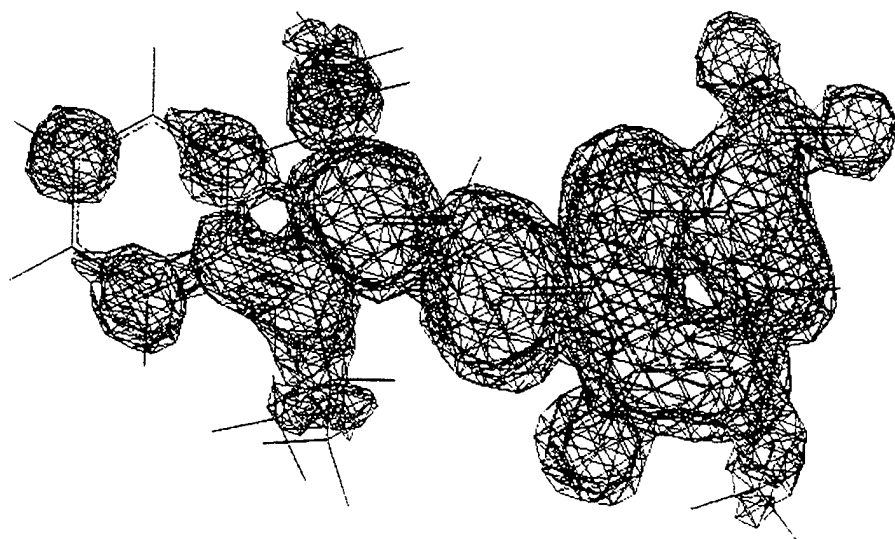


Figure 3.16: The LUMO of the indoline-benzopyran merocyanine.

### 3.1.3 Spectral Shifts

It is the goal of this research to engineer organic chromophores in which the absorption peaks are red shifted as much as possible. One reason is that chromophores are commonly placed in polar solvents in order to reduce the fading rate, thus maintaining the colored form as long as possible. Unfortunately, due to solvatochromic affects, polar solvents tend to blue shift the absorption peaks of the merocyanine. Therefore, red shifted chromophores will yield optimal colorization by maximizing both position of the peak absorption and the stability of the merocyanine. The primary thrust of this research is to better understand and refine the optical absorption spectrum of the merocyanine form.

According to quantum mechanics, shifts of an absorption spectrum may be achieved by considering first order perturbations of the excitation from occupied orbital  $m$  to virtual orbital  $n$ ,  $m \Rightarrow n$ . The resultant equations show that shifts in the electronic absorption spectra may be achieved in two ways. First, spectral shifts are a function of substituent choice and placement.<sup>37</sup>

$$\delta\Delta E_{m \Rightarrow n} = -\Delta P_{ii} \delta h_i \quad (3.1)$$

$\Delta E_{m \Rightarrow n}$  is the difference in energy between molecular orbitals  $m$  and  $n$ . Molecular orbital  $m$  is an occupied (bonding) orbital and  $n$  is a virtual (anti-bonding) orbital.  $\Delta P_{ii}$  is the difference (between states  $n$  and  $m$ ) of the total  $\pi$  electron density around atom  $i$ .  $\delta h_i$  is the correction term of the Coulomb integral that accounts for atoms or groups of atoms other than carbon. The value of  $\delta h_i$  is positive for atoms more electronegative than carbon or when an electron withdrawing substituent is introduced at atom  $i$ . Table 3.2 shows how the substituent can alter the absorption spectrum. Bathochromic shifts are movements of peaks in the absorption spectrum to longer wavelengths while hypsochromic shifts are to shorter wavelengths.

| Variable                 | $\Delta P_{ij}$ is negative | $\Delta P_{ij}$ is positive |
|--------------------------|-----------------------------|-----------------------------|
| $\delta h_j$ is negative | Bathochromic shift          | Hypsochromic shift          |
| $\delta h_j$ is positive | Hypsochromic shift          | Bathochromic shift          |

Table 3.2: The effects of substituents on the absorption spectra.

The absorption spectra may also be shifted by bond rotation.<sup>38</sup>

$$\delta \Delta E_{m \rightarrow n} = -2 \Delta P_{ij} \delta k_{ij} \quad (3.2)$$

$\Delta P_{ij}$  is the change in bond order of the bond connecting atoms i and j. The value of  $\Delta P_{ij}$  is negative for rotation about essentially double bonds and positive for rotation about essentially single bonds.  $k_{ij}$  is a correction to the resonance integral to account for the change in geometry. The value of  $k_{ij}$  is a maximum when the two orbitals are parallel and decreases as bond i-j is rotated. Table 3.3 shows how rotation can alter the absorption spectra.

| Variable                    | $\Delta P_{ij}$ is negative | $\Delta P_{ij}$ is positive |
|-----------------------------|-----------------------------|-----------------------------|
| $\delta k_{ij}$ is negative | Bathochromic shift          | Hypsochromic shift          |
| $\delta k_{ij}$ is positive | Hypsochromic shift          | Bathochromic shift          |

Table 3.3: The effects of geometry on the absorption spectra.

Figure 3.17 shows the atomic and bond numbering scheme of the unsubstituted indoline-benzopyran merocyanine. As previously stated, the strongest electronic transition in the merocyanine is  $g \rightarrow 1$ . Therefore, the  $P_{ij}$  values shown in table 3.4 were computed

for this transition. Table 3.4, in conjunction with table 3.2, shows that large bathochromic shifts may be achieved by attaching the appropriate substituent to either atom 2 or 3. Although atom 4 has a large  $|\Delta P_{ij}|$  value it is unavailable for substitution. The attachment of an electron withdrawing substituent ( $\delta h_i$  positive) to atom number 3 ( $\Delta P_{ij}$  positive) should produce a bathochromic shift. Figure 3.18, however, shows that when chlorine is attached to position 3 the expected bathochromic shift does not occur.

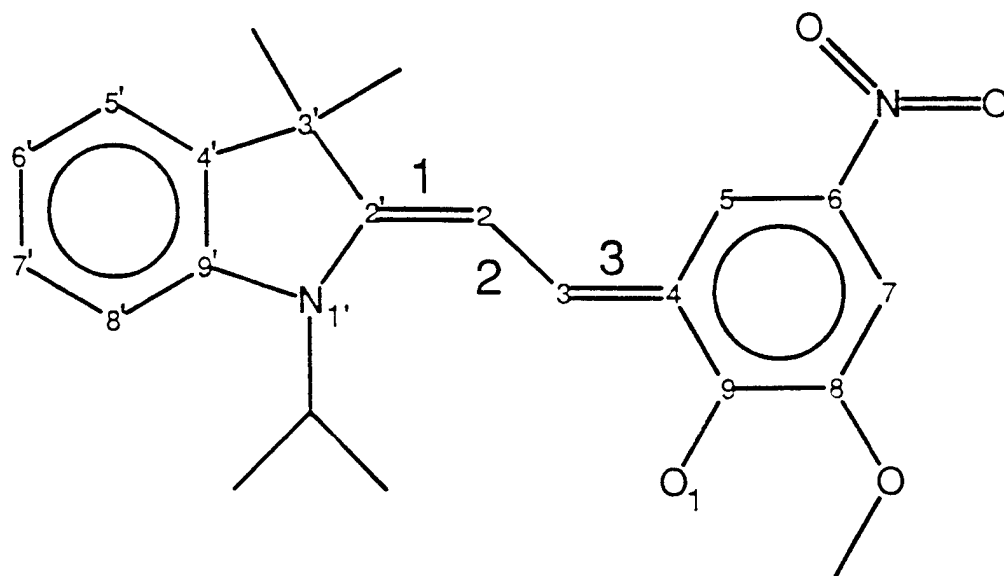


Figure 3.17: The numbering of the trans-cis indoline-benzopyran merocyanine.

| Atomic Number<br>(Type) | $\Delta P_{ii}$ |
|-------------------------|-----------------|
| 3 (C)                   | 0.242           |
| 4 (C)                   | -0.145          |
| 2 (C)                   | -0.141          |
| 5 (C)                   | 0.130           |
| 2' (C)                  | 0.127           |
| 6 (C)                   | -0.088          |
| 1 (O)                   | -0.088          |
| 1' (N)                  | -0.072          |
| 8 (C)                   | -0.033          |
| 7 (C)                   | 0.025           |
| 9 (C)                   | 0.021           |
| 4' (C)                  | -0.019          |
| 6' (C)                  | -0.015          |
| 9' (C)                  | -0.012          |
| 7' (C)                  | -0.006          |
| 8' (C)                  | -0.005          |
| 5' (C)                  | 0.003           |
| 3' (C)                  | -0.002          |

Table 6.  $\Delta P_{ii}$  values of the indoline-benzopyran merocyanine in order of decreasing  $|\Delta P_{ii}|$ .



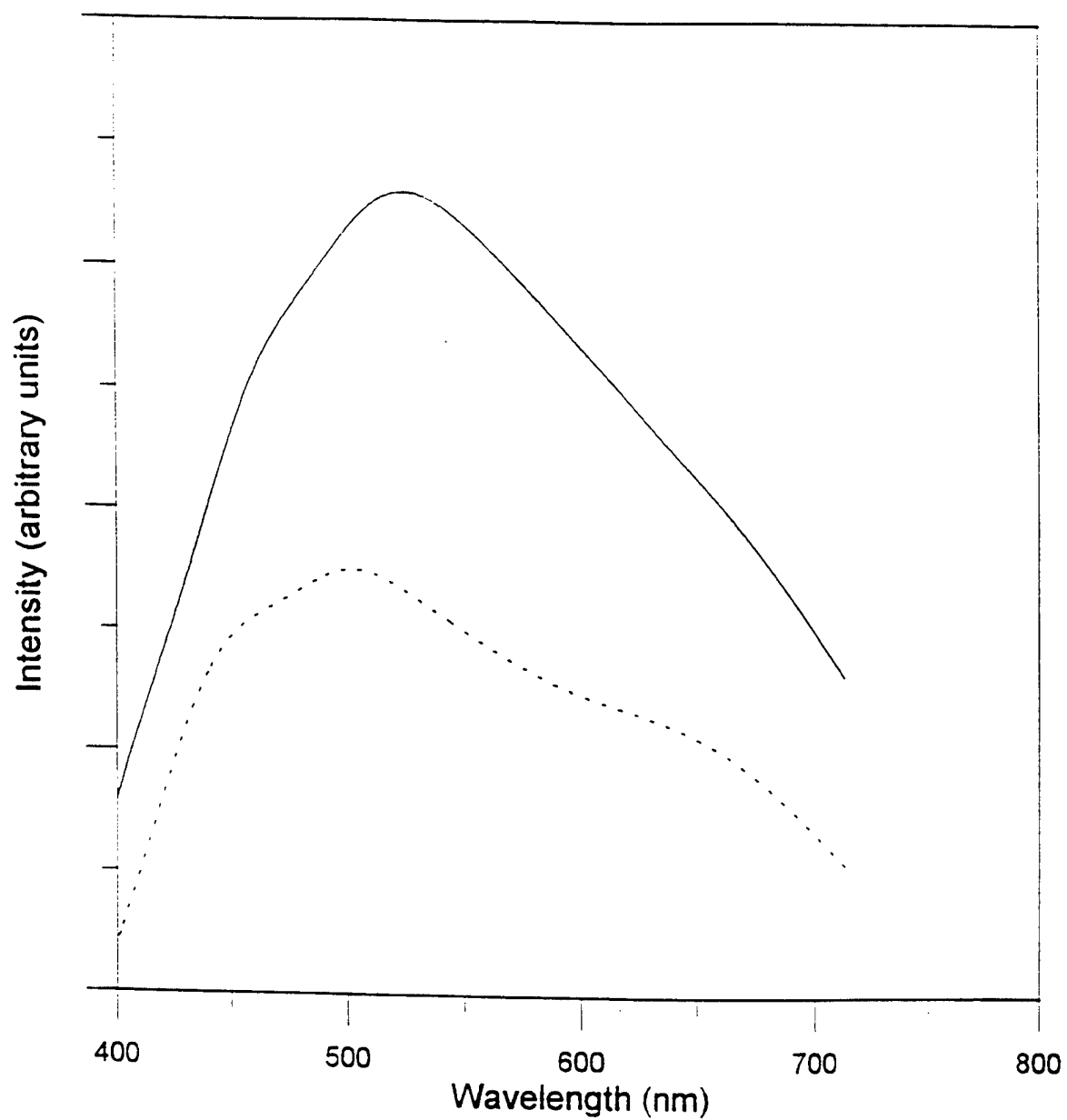


Figure 3.18: The computed spectra of the Cl substituted (----) and unsubstituted (—) indoline-benzopyran merocyanine.

Recall that BOTH substitution and bond twisting can result in either bathochromic OR hypsochromic shifts. Therefore the spectrum can be understood by examining the molecular geometry of the minimized chlorine substituted merocyanine. Bonds one and three of the unsubstituted merocyanine are essentially double, having bond orders of 1.55. Bond two is essentially single having a bond order of 1.18. The torsion angles about the three delocalized bonds of the optimized chlorine substituted merocyanine are seen in table 3.5. Although equation 3.1 predicts that a bathochromic shift will result from the substitution of an electron withdrawing substituent at atom 3, equation 3.2 shows that the  $47^\circ$  twist about the single bond will produce a hypsochromic shift. The same geometric effect was seen when the electron withdrawing substituent OH was placed at the same position. Due to the factor of two present in equation 3.2, departures from planarity dominate the substituent effects embodied in equation 3.1. This demonstrates the interdependence of equations 3.1 and 3.2. The placement of electron withdrawing substituents may not produced bathochromic shifts because of the induced rotation about bond two. A more extensive list of electron withdrawing substituents needs to be examined to rule out their ability to produce bathochromic shifts in the absorption spectra of the indoline-benzopyran.

| Torsion angle<br>Substituent | $\phi_1$    | $\phi_2$    | $\phi_3$   |
|------------------------------|-------------|-------------|------------|
| H                            | $176^\circ$ | $179^\circ$ | $1^\circ$  |
| Cl                           | $175^\circ$ | $133^\circ$ | $-4^\circ$ |
| OH                           | $174^\circ$ | $144^\circ$ | $-4^\circ$ |

Table 3.5: Torsion angles of electron withdrawing substituted merocyanine

An alternative way to produce large bathochromic shifts in the absorption spectrum is by placing an electron donating substituent ( $\delta h_i$  negative) on atom 2 ( $\Delta P_{ii}$  negative). The substituents examined in these spectroscopic calculations were H, OCH<sub>3</sub> and thiophene (in order of electron donating ability). The spectral effects of attaching these substituents to atom 2 are seen in figure 3.19. Specifically, the strongest (highest oscillator strength  $f_{mn} \approx 1.0$ ) transition occurs at 461 nm for the unsubstituted, 480 nm for the OCH<sub>3</sub> substituted and 473 nm for the thiophene substituted merocyanines. There are a number of weaker transitions ( $f_{mn} \approx 0.4$ ) located at slightly higher wavelengths than the main transition. The spectrum thus appears red shifted relative to the main transition. Although thiophene is more electron donating than OCH<sub>3</sub>, geometric effects again intervene to determine the positions of the absorption spectra. Rotation about bonds one and three will produce bathochromic shifts because these are essentially double bonds. On the other hand, rotation about bond two, which is essentially single, produces hypsochromic shifts. Table 3.6 lists the torsion angles of these systems.

| Torsion angle<br>Substituent | $\phi_1$ | $\phi_2$ | $\phi_3$ |
|------------------------------|----------|----------|----------|
| H                            | 176°     | 179°     | 1°       |
| OCH <sub>3</sub>             | 159°     | 176°     | 6°       |
| Thiophene                    | 165°     | 162°     | -2°      |

Table 3.6: The torsions of substituted trans-cis indoline-benzopyran merocyanines.

**THIS PAGE LEFT INTENTIONALLY BLANK**

The deviations from planarity of bonds one and three complement the bathochromic shifts due to the OCH<sub>3</sub> substituent. Because there is only a small rotation about bond two, this spectral shift is maximized. The thiophene substituted merocyanine, however, exhibits less rotation about bonds one and three, but more rotation about bond two. These two factors override the strong electron donating ability of thiophene, thereby displacing the absorption peak to a shorter wavelength than that calculated for the OCH<sub>3</sub> substituted merocyanine.

The stabilities of the four isomers of the substituted indoline-benzopyran merocyanine were also examined (see table 3.7). The trans-cis isomer (already addressed) is the most stable form in each case, followed closely by the cis-cis. The absorption spectrum of the cis-cis form is thus also worth examining. The higher heats of formation of the trans-trans and cis-trans arise largely from the unfavorable interactions between the oxygen and the substituent. Because these isomers are not thermodynamically favored, they will not be examined in detail.

| Substituent<br>Isomer | H                | OCH <sub>3</sub> | Thiophene        |
|-----------------------|------------------|------------------|------------------|
| trans-cis             | 20.06 (kcal/mol) | -8.81 (kcal/mol) | 70.08 (kcal/mol) |
| cis-cis               | 20.77 (kcal/mol) | -8.60 (kcal/mol) | 73.50 (kcal/mol) |
| trans-trans           | 21.14 (kcal/mol) | -3.38 (kcal/mol) | 75.76 (kcal/mol) |
| cis-trans             | 21.80 (kcal/mol) | -2.01 (kcal/mol) | 80.55 (kcal/mol) |

Table 3.7: Heats of formation of the substituted indoline-benzopyran isomers.

The absorption spectra of the substituted cis-cis indoline-benzopyran merocyanines follow the expected trend, with the peak absorption of the OCH<sub>3</sub> substituted merocyanine occurring at 470 nm and that of the thiophene substituted merocyanine occurring at 475 nm. The difference in the relative positions of the peaks of the trans-cis substituted merocyanines (H, thiophene and OCH<sub>3</sub>) and the cis-cis isomers (H, thiophene and OCH<sub>3</sub>) can be understood by examining the molecular geometries. The torsion angles of both the trans-cis and the cis-cis isomers are given in table 3.8. The hypsochromic shift of the OCH<sub>3</sub> substituted cis-cis isomer relative to its trans-cis counterpart is due to the return to planarity of  $\phi_1$  and simultaneous loss of planarity of  $\phi_2$ . These changes in  $\phi_1$  and  $\phi_2$  both cause hypsochromic shifts. In the thiophene-substituted cis-cis isomer, both  $\phi_1$  and  $\phi_2$  are nearer to their planar values compared to the trans-cis isomer. Thus the hypsochromic shift produced by the change in  $\phi_1$  is counteracted by the bathochromic shift produced by the change in  $\phi_2$ . This explains the relative positions of the trans-cis and cis-cis substituted absorption maxima.

| Torsion angle<br>Substituent | $\phi_1$   | $\phi_2$    | $\phi_3$  |
|------------------------------|------------|-------------|-----------|
| H                            | -4° (176°) | 178° (179°) | 1° (1°)   |
| OCH <sub>3</sub>             | 6° (159°)  | 162° (176°) | 6° (6°)   |
| Thiophene                    | -3° (165°) | 179° (162°) | -2° (-2°) |

Table 3.8: The torsions of substituted cis-cis indoline-benzopyran merocyanines. The torsions of the trans-cis isomer are shown in parentheses.

The absorption spectra of substituted spiropyrans (figure 3.20) isolates the effects of substitution because there is no bond rotation. The main transition of the unsubstituted spiropyran occurs at 272 nm, for the  $\text{OCH}_3$  substituted spiropyran it occurs at 279 nm, and for the thiophene substituted spiropyran it occurs at 292 nm. This is precisely the order predicted by equation 3.1. Further, in the unsubstituted spiropyran the transition which causes the carbon-oxygen bond to break is a result of the  $g \rightarrow 5$  excitation, while it is the  $g \rightarrow 4$  excitation in the  $\text{OCH}_3$  substituted spiropyran and the  $g \rightarrow 3$  excitation in the thiophene substituted spiropyran. Electron donating substituents stabilize the anti-bonding orbitals compared to less electron donating substituents. The stabilization of anti-bonding orbitals leads to a lower energy transition and hence bathochromic shifts in the absorption spectrum.

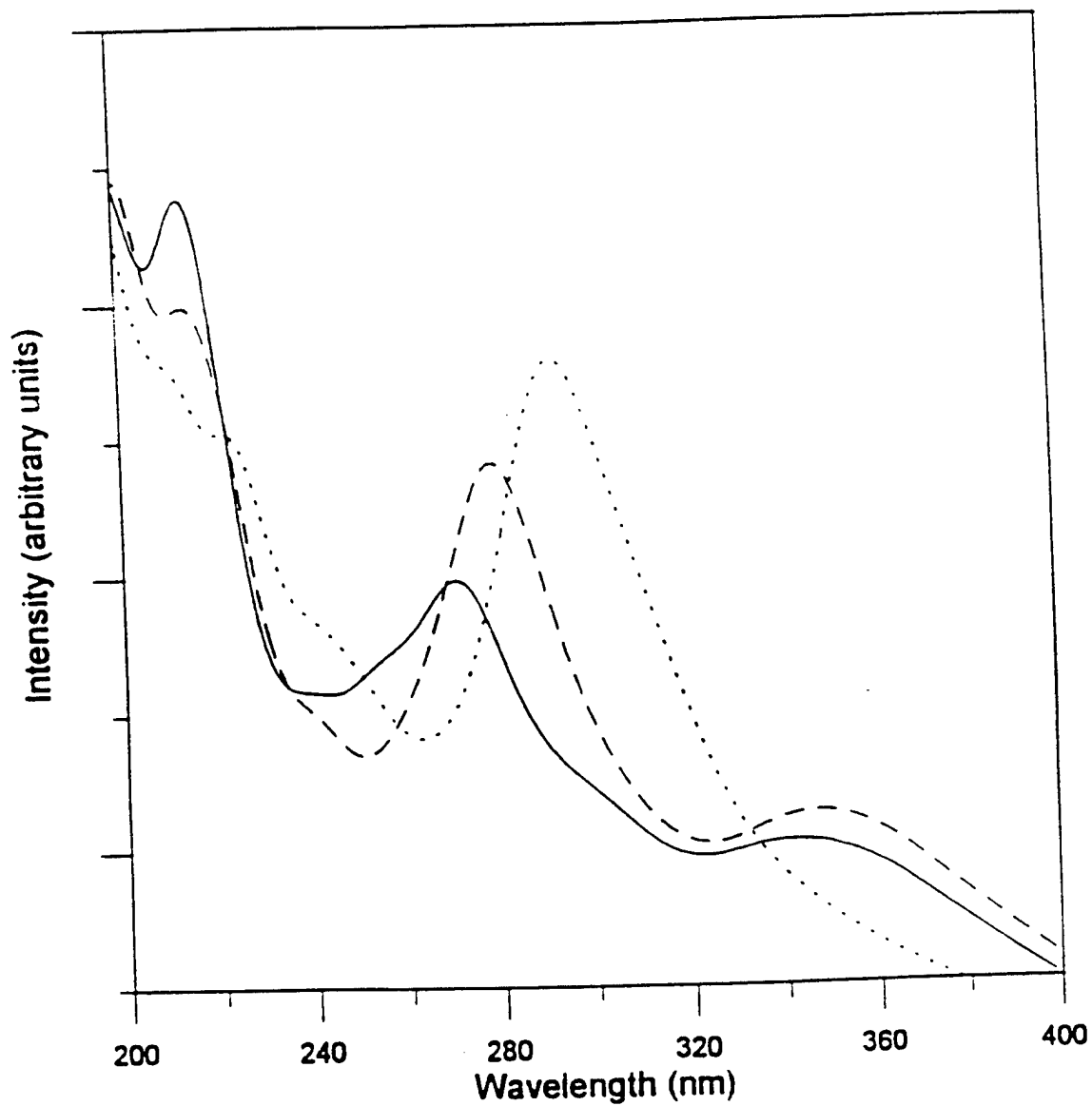


Figure 3.20: Spectra of substituted (H(—), OCH<sub>3</sub>(- - -) and thiophene(·····)) indoline-spiro-benzopyrans.



### 3.1.4 The Benzothiazoline-Benzopyran

Along with the indoline-benzopyran, the electronic spectra of the two forms of benzothiazoline-benzopyran are of interest. Removing the two methyl groups attached to atom 3' and replacing this carbon atom with a sulfur atom transforms the indoline-spiro-benzopyran into the benzothiazoline-spiro-benzopyran. Equation 3.1 predicts that this transformation should not change the absorption spectrum substantially for two reasons. First, atom 3' is insensitive to atomic substitution or substituent placement by virtue of its extremely small  $|\Delta P_{ii}|$  value of -0.002. Secondly, the electronegativity of both sulfur and carbon is 2.5, and  $\delta h_i$  is thus zero.<sup>39</sup>

The spectra of the merocyanine forms of the substituted trans-cis indoline-benzopyran and benzothiazoline-benzopyran are now compared. Figure 3.21 shows the atomic numbering scheme and table 3.9 shows the  $\Delta P_{ii}$  values for the benzothiazoline-benzopyran merocyanine. The placement of electron withdrawing substituents on atom 3 does not produce bathochromic shifts because of the same bond twisting which occurred in the indoline-benzopyran. The effects on the spectrum of placing electron donating substituents placed at position 2 of the benzothiazoline-benzopyran is now examined. The torsion angles about the three central bonds of the substituted indoline and benzothiazoline systems differ by less than 1°. Therefore no shift in the spectra due to bond twisting should arise. Attaching the same electron donating substituents should produce the same bathochromic shifts as in the indoline-benzopyran systems. Figure 3.22 shows that the spectra of the substituted benzothiazoline-benzopyran merocyanine are indeed very similar to those of the indoline-benzopyran merocyanine shown in figure 3.19.

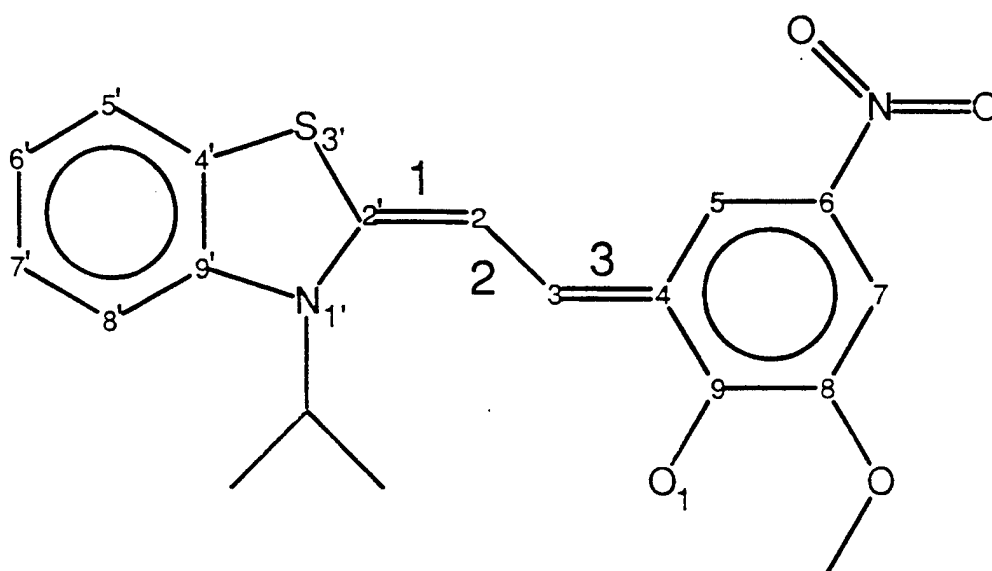


Figure 3.21: The numbering of the benzothiazoline-benzopyran.

| Atomic Number<br>(Type) | $\Delta P_{ii}$ |
|-------------------------|-----------------|
| 3 (C)                   | 0.240           |
| 2 (C)                   | -0.137          |
| 4 (C)                   | -0.135          |
| 2' (C)                  | 0.134           |
| 5 (C)                   | 0.121           |
| 6 (C)                   | -0.081          |
| 1 (O)                   | -0.080          |
| 1' (N)                  | -0.069          |
| 8 (C)                   | -0.030          |
| 7 (C)                   | 0.026           |
| 9 (C)                   | 0.024           |
| 4' (C)                  | -0.022          |
| 3' (S)                  | -0.020          |
| 6' (C)                  | -0.016          |
| 9' (C)                  | -0.015          |
| 7' (C)                  | -0.008          |
| 8' (C)                  | -0.004          |
| 5' (C)                  | 0.003           |

Table 3.9:  $\Delta P_{ii}$  values for the benzothiazoline-benzopyran in order of decreasing  $|\Delta P_{ii}|$ .

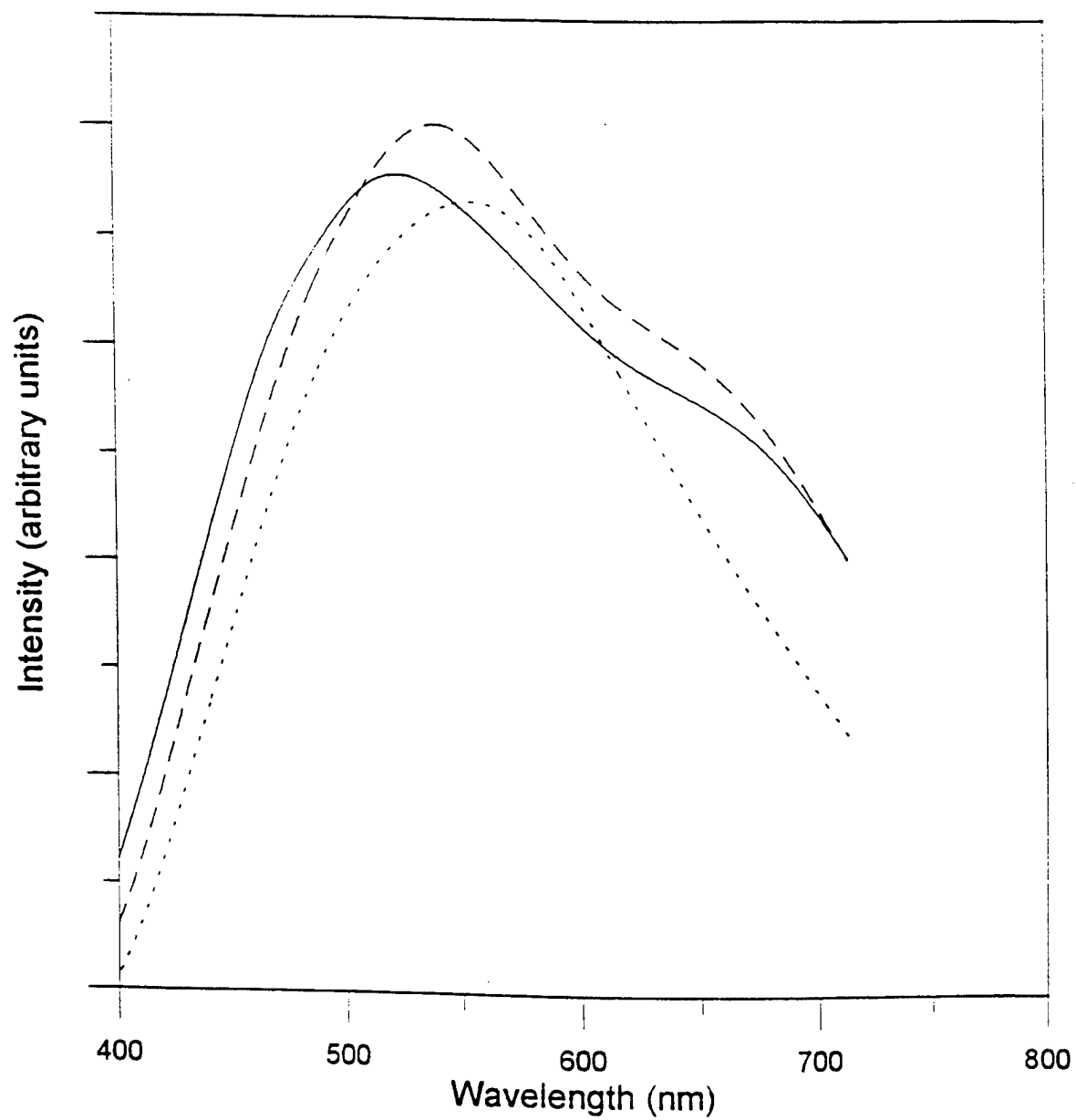


Figure 3.22: The spectra of substituted (H(—), OCH<sub>3</sub>(- -) and thiophene(.....)) trans-cis benzothiazoline-benzopyrans.

## 3.2 Force Field Modeling

Before force field calculations (either molecular mechanics or molecular dynamics) can be carried out, the proper choice of force field parameters must be made. The TRIPOS force field, which is parameterized for use with general organic molecules, is the basic force field used to examine the organic photochromes in this research. The force field parameters to be used with the merocyanine form of the photochrome must be examined carefully. Along the three bonds that connect the indoline and benzopyran fragments of the merocyanine (bonds one, two and three) there is substantial electron delocalization. The manifestation of delocalization in these bonds is that in the minimum energy structure their bond orders are intermediate between those of single and double bonds, 1.55, 1.18 and 1.55 respectively. Further, these bond orders depend on the torsion angles around these bonds. The TRIPOS force field can only describe these bonds as being immutably either single or double. The use of such parameters would therefore lead to unrealistic bending and twisting in this region of the molecule.

### 3.2.1 Force Field Parameterization

Choosing the correct parameters requires that either experimental data or accurate computational data be obtained for the specific system in question. Generation of the potential energy map of merocyanine using MOPAC is the best method of obtaining data from which improved force field parameters can be extracted. Various conformations of the unsubstituted trans-cis indoline-benzopyran merocyanine were formed by independently rotating the three delocalized bonds (bonds 1, 2 and 3) in thirty degree increments over a 360° range. These torsion angles,  $\phi_1$ ,  $\phi_2$ , and  $\phi_3$ , were fixed while the rest of the geometry was optimized using MOPAC and the AM1 parameterization. This was done for each of the 12<sup>3</sup> conformations.

Energy surfaces of the indoline-benzopyran merocyanine were constructed from the molecular heats of formation. Figure 3.23 shows the surface for rotation about bonds 1 and 3 while  $\phi_2$  was fixed at  $180^\circ$ . This surface shows that rotation by  $180^\circ$  about bonds 1, 3 or both gives the four low energy isomers of the merocyanine discussed in the previous section.

Rotation about bonds 2 and 3 with  $\phi_1 = 0^\circ$  yields the potential energy surface shown in figure 3.24. Unlike rotations about bonds 1 and 3, rotation about bond 2 does not have two-fold symmetry. This is due to the large steric interactions which can occur between the indoline and benzopyran segments when this bond is rotated. The peaks on this energy surface are 50 kcal / mol. When the interaction between the two ring systems was minimized i.e. when bond 2 remained unrotated, the peaks were 29 kcal/mol. The remaining energy surfaces largely redisplay the data shown in figures 3.23 and 3.24.

The bond orders for these bonds were also calculated. Rotations about the three bonds connecting the indoline and benzopyran portions of the merocyanine dictate the degree of conjugation (i.e., electronic delocalization) present in the merocyanine. Bond orders are a convenient way of quantifying the electron density that exists between atoms. It is this electron density that dictates the strength (i.e. the length and the resistance to twisting) of the bond. The bond order between two atoms is a measure of the overlap between the two atomic  $\pi$  orbitals. As such, the bond orders vary roughly as a cosine function as the bond is rotated.

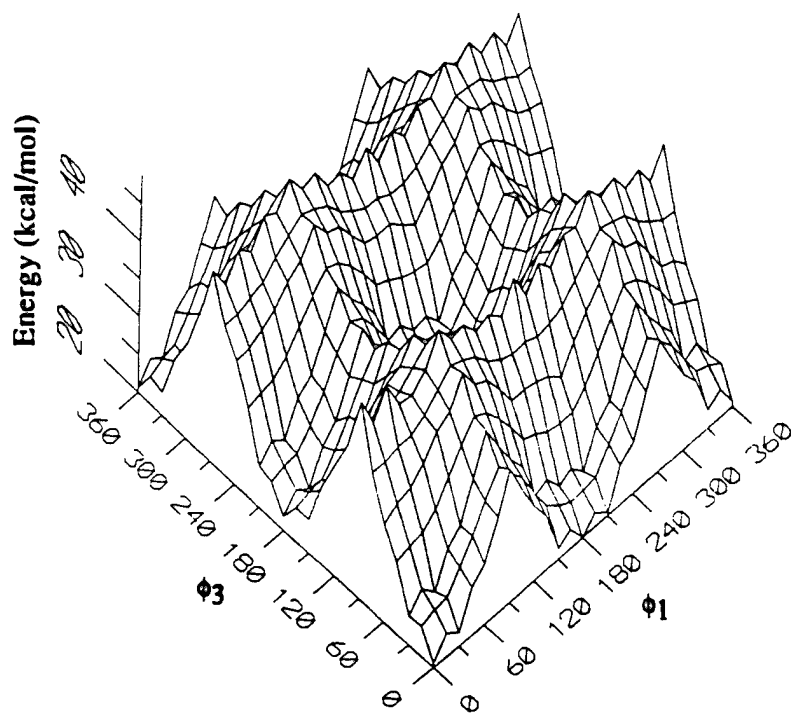


Figure 3.23: Potential energy surface of merocyanine.  $\phi_2 = 180^\circ$ .

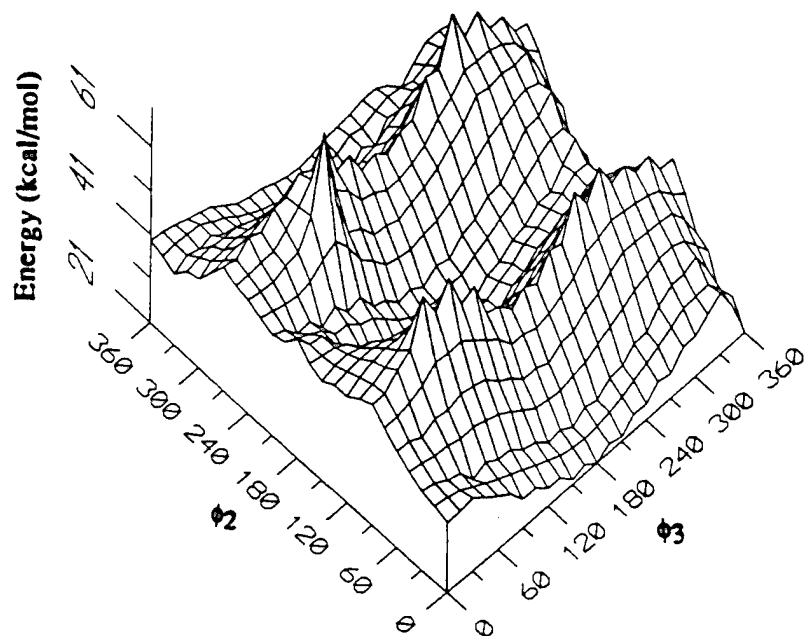


Figure 3.24: Potential energy surface of merocyanine.  $\phi_1 = 0^\circ$ .

Figures 3.25, 3.26 and 3.27 show the bond orders of bonds one, two and three which correspond to the  $\phi_2 = 180^\circ$  potential energy surface (figure 3.23). The bond orders of bonds one and three vary from 1.0 to 1.6 while bond two varies from 1.2 to 1.8. Bonds one, two and three may exhibit double-single-double bond characteristics (1.55, 1.18 and 1.55, respectively), single-double-single bond characteristics (1.01, 1.82 and 1.01, respectively) or aromatic characteristics (1.35, 1.36 and 1.38 respectively). When in a planar conformation the bond orders are 1.55, 1.18, and 1.55 respectively.

Comparing the potential energy surface when  $\phi_2 = 180^\circ$  (figure 3.23) to the corresponding bond order surfaces yields two conclusions. When the conformational energy of the merocyanine is low the bond orders of bonds 1 and 3 are essentially double with respect to bond 2, thus adopting an essential double-single-double (2-1-2) structure. The reverse is also true: when the energy is high, a single-double-single (1-2-1) bond ordering appears.

Transforming this quantum mechanical result into a form useful for classical calculations will allow large complex systems to be investigated computationally. Classically, bonds are described as being either fully single or double and remain so for the duration of the calculation. As seen above, the nature of the delocalization which occurs across bonds one, two and three of the merocyanine is dependent upon the torsion angles about these bonds. A useful force field for the merocyanine must allow for the conformational flexibility which results from these changes in bond order and vice versa (i.e., the changes in bond order that occur because of this flexibility). Thus to model transitions between isomers of the merocyanine, various force fields would have to be applied during MM or MD calculations, depending upon the position of the conformer upon the potential energy surface. Likewise, in order to model the open/closed transition classically, an adaptive force field would need to be employed to account for the electronic changes which occur in the chromophore during bond dissociation or formation.



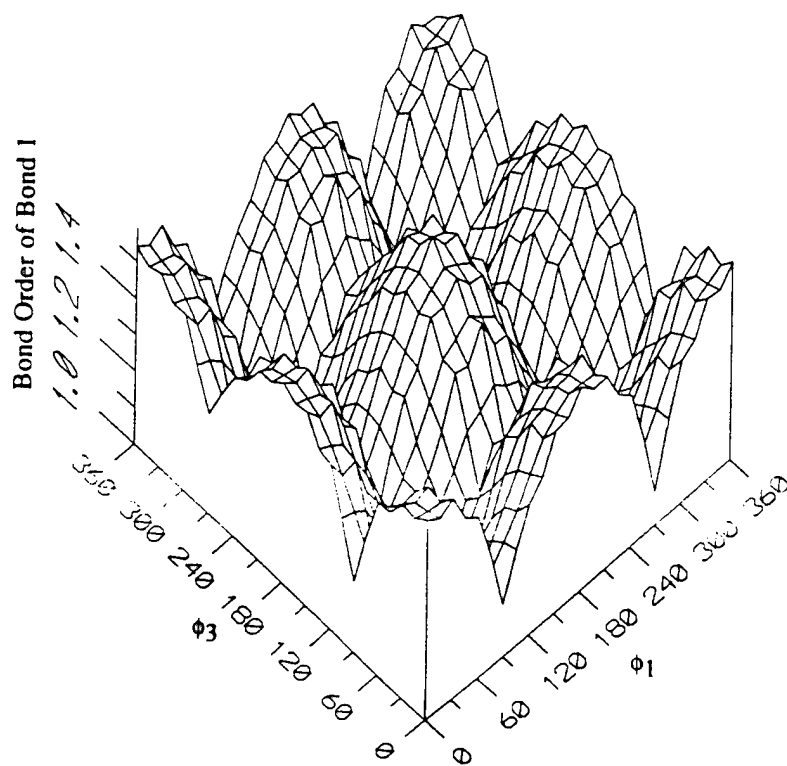


Figure 3.25: Bond order surface of bond one.  $\phi_2 = 180^\circ$ .

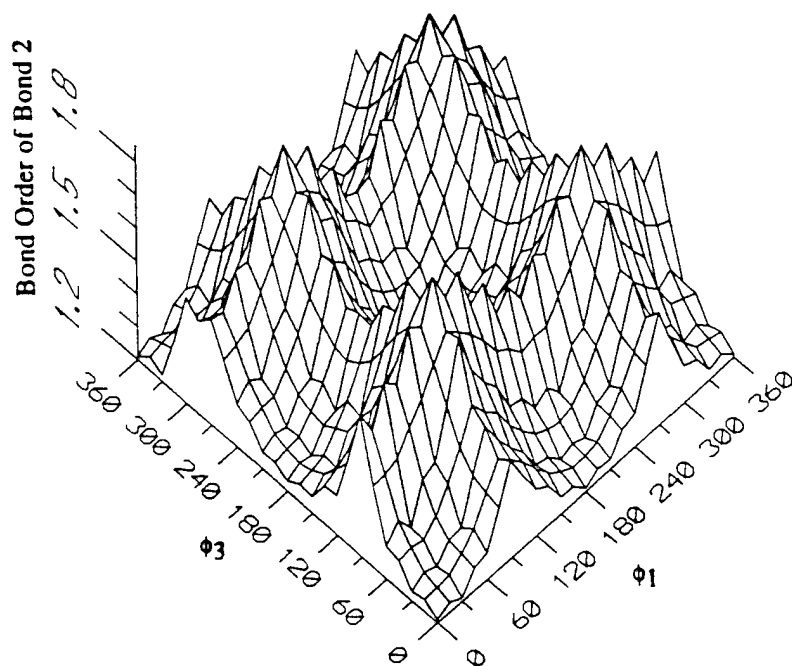


Figure 3.26: Bond order surface of bond two.  $\phi_2 = 180^\circ$ .

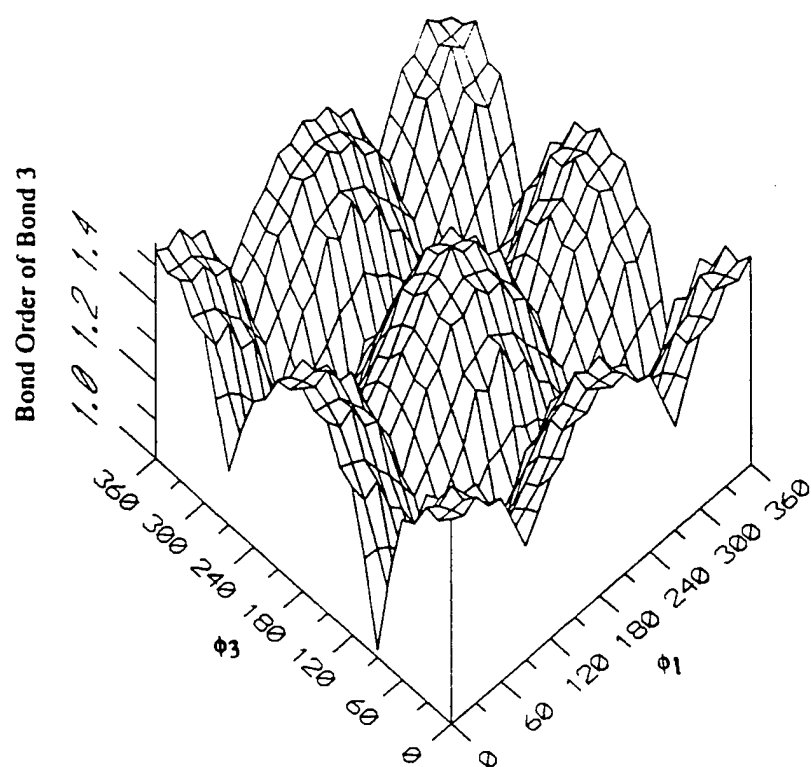


Figure 3.27: Bond order surface of bond three.  $\phi_2 = 180^\circ$ .

As a first step toward dealing with the complexity of this situation, two force fields were developed to allow classical calculations for the merocyanine molecule to be made. The two force fields are the double-single-double (2-1-2) force field, in which there is greater electron density along bonds 1 and 3 than along bond 2, and the single-double-single (1-2-1) force field, where bond 2 has greater electron density than bonds 1 and 3. These represent the two extremes of behavior that might be expected. Until a method of prescribing an adaptive force field during molecular simulations is developed, these limiting behaviors can yield useful insights.

To achieve a classical representation of the quantum mechanical potential energy surface, molecular mechanics was used to evaluate the classical energies of the MOPAC optimized molecules. The charges calculated by MOPAC for the lowest energy merocyanine were used to allow the inclusion of electrostatics in the classical energy evaluation. A fixed dielectric constant of 1.0 was used along with a 1-4 energy term scaling factor of 0.5, a non-bonded cutoff of 8Å and a van der Waals radius scaling factor of 0.7. During molecular mechanics optimizations, rotations about the three central bonds were constrained (paralleling the MOPAC calculations) by imposing a rotation barrier of 30 kcal/mol degree<sup>2</sup> to these torsion angles.

$$E_{\text{tor. constraint}} = 1 / 2 k^t ( \phi - \phi^0 )^2 \quad (3.3)$$

$\phi$  is the torsion angle,  $\phi^0$  is the proscribed value of the torsion angle and  $k^t$  is the barrier to rotation. This constraint added less than 0.1 kcal/mol to the energy of the molecule, thus effectively constraining the angles. The energy of each conformation was then minimized using the steepest descents method, followed by the Powell method. A 0.05 kcal/mol energy convergence was used as the termination criterion for both iterative methods. Selected TRIPOS force field parameters were then adjusted until agreement

between the classical energy profile and the MOPAC potential energy curve (in one dimension) was achieved.

The 2-1-2 force field was found by constraining  $\phi_1$  and  $\phi_3$  to zero degrees while rotating about bond two, followed by the aforementioned minimization procedure. MOPAC results show that along this curve the bond orders are double-single-double in nature (figure 3.28). The force field parameters were modified until agreement with the MOPAC potential energy curve was achieved. Table 3.10 lists these modified values (only modified parameters have been listed). The small modification of the 6-12 hydrogen potential was necessary to alleviate unrealistically large steric interactions which occur when methyl groups are attached to the indoline carbon. The quantum mechanical (MOPAC) and the classical (modified 2-1-2 force field) energies are in good agreement (figure 3.29).

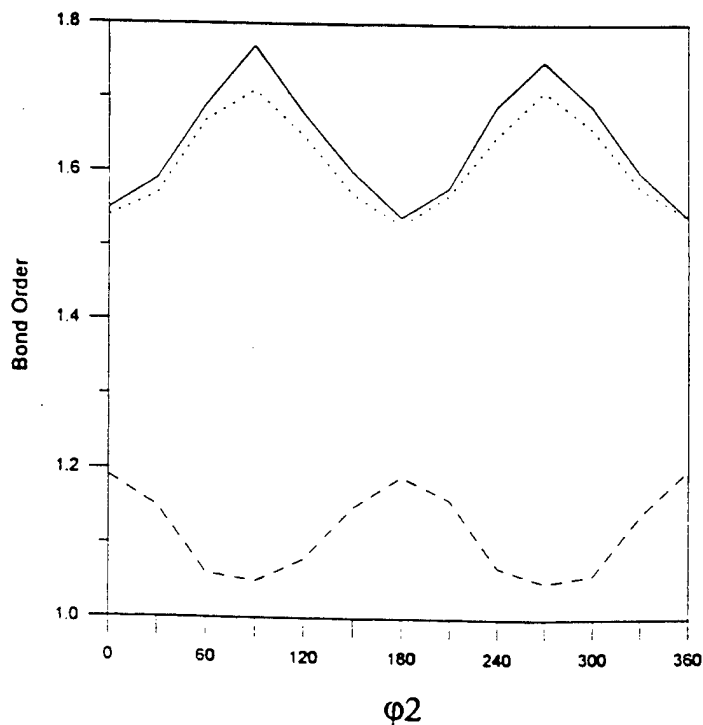


Figure 3.28: Bond orders of bond 1(—), 2(- -) and 3(---).  $\phi_1=\phi_3=0^\circ$ .

### BOND STRETCHING

| Atom i | Atom j | Bond type | $d_{ij}^0$ (Å) | k (kcal/mol Å <sup>2</sup> ) |
|--------|--------|-----------|----------------|------------------------------|
| C2     | C2     | 2         | 1.375 (1.335)  | 1340                         |
| C2     | C2     | 1         | 1.411 (1.47)   | 700                          |
| Car    | Car    | ar        | 1.395 (1.395)  | 700 (1400)                   |
| C2     | N2     | 1         | 1.396 (1.444)  | 1300                         |
| Car    | N2     | 1         | 1.417 (1.346)  | 1305.94                      |
| Car    | Npl3   | 1         | 1.481 (1.35)   | 1306                         |
| C2     | Car    | 2         | 1.375 (*)      | 1340                         |
| Car    | O3     | 2         | 1.244 (*)      | 600                          |

### Angle Bending

| Atom i | Atom j | Atom k | Theta        | k(kcal/moldeg <sup>2</sup> ) |
|--------|--------|--------|--------------|------------------------------|
| C2     | C2     | C2     | 128 (121.7)  | 0.018                        |
| C2     | C2     | Car    | 125 (120)    | 0.026                        |
| C2     | C2     | N2     | 130 (120)    | 0.024                        |
| C3     | C2     | N2     | 109 (118)    | 0.02                         |
| C2     | C3     | Car    | 102 (109.47) | 0.018                        |
| C3     | Car    | Car    | 109 (120)    | 0.024                        |
| Car    | Car    | N2     | 110 (120)    | 0.04                         |
| C2     | N2     | C3     | 124 (110)    | 0.082                        |
| C2     | N2     | Car    | 109 (123)    | 0.08                         |

### Torsional

| Atom i | Atom j | Atom k | Atom l | Bond type | k(kcal/moldeg <sup>2</sup> ) | s  |
|--------|--------|--------|--------|-----------|------------------------------|----|
| *      | C2     | C2     | *      | 2         | 9.5 (12.5)                   | -2 |
| *      | C2     | C2     | *      | 1         | 4 (1.424)                    | -2 |
| *      | C2     | Car    | *      | 2         | 9.5 (12.5)                   | -2 |

### 6 - 12 Potential

| Atom | r (Å)      | k (kcal/mol) |
|------|------------|--------------|
| H    | 1.45 (1.5) | 0.042        |

\* denotes wildcard entries.

Table 3.10: Modified TRIPOS 2-1-2 force field parameters. Values in parentheses are the original TRIPOS values.

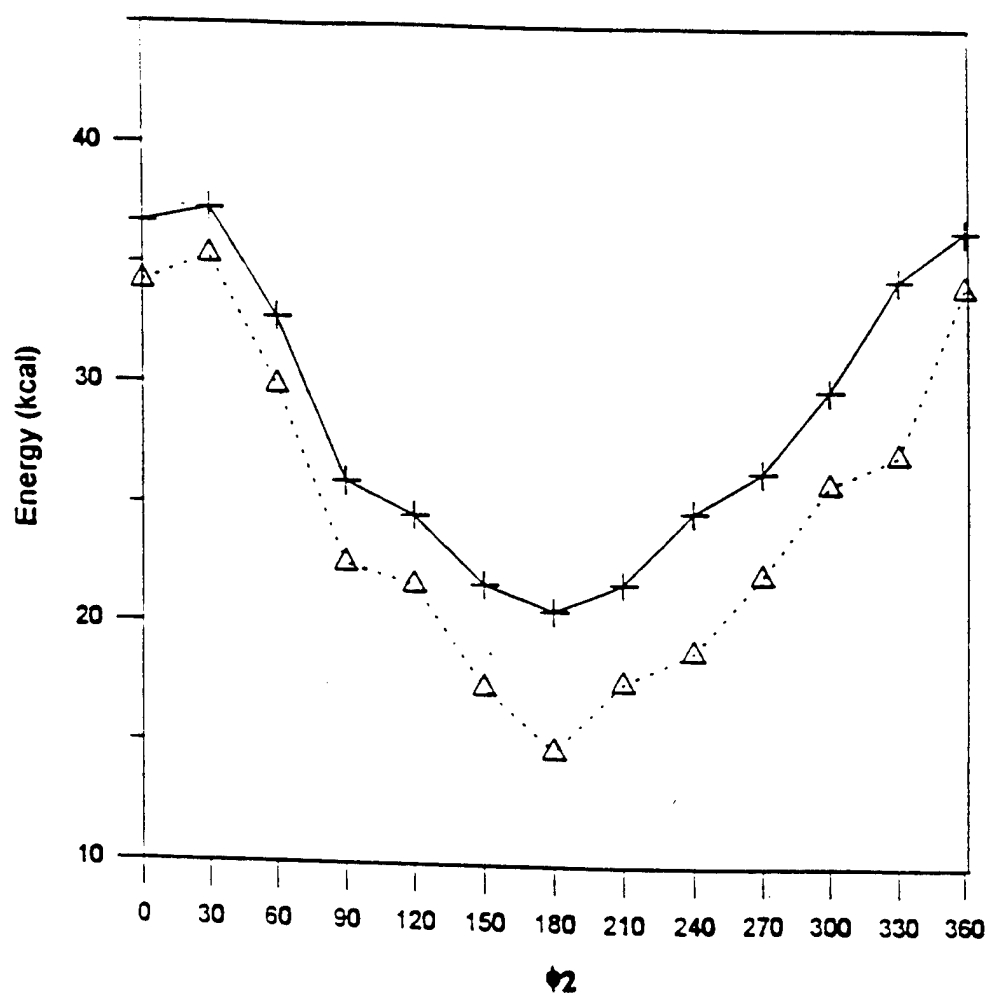


Figure 3.29: Comparison of the energies calculated by the modified 2-1-2 force field (---) and MOPAC (—).

The 1-2-1 force field was then constructed by constraining  $\phi_1$  to  $90^\circ$  and  $\phi_2$  to  $180^\circ$  while rotating about bond three. Along this curve, the bond orders are single-double-single in nature (figure 3.30). The modified values of the TRIPOS force field parameters are listed in table 3.11. The ability of this force field to reproduce quantum mechanical results is seen in figure 3.31. Rotations about bond 1 while constraining  $\phi_3$  to  $90^\circ$  and  $\phi_2$  to  $180^\circ$  would be expected to yield very similar results.

The force field parameters which most directly model the electron delocalization are the bond stretching and torsional terms. For the 2-1-2 force field (bond orders of 1.55-1.18-1.55) the length of the double bond was decreased from its purely double bond value given by TRIPOS. Similarly the length of the single bond was increased from its given TRIPOS value. The torsional barrier was also decreased for the double bonds relative to the pure state given by TRIPOS while the torsional barrier was increased for the single bonds. In the 1-2-1 force field these bond stretching and torsional parameters are reversed to account for the migration of electron density from bonds one and three to bond two. Other force field parameters were adjusted to provide agreement between the geometries of the hypothetical (parameterized) molecule and that obtained by MOPAC.

The modified force fields yield energy barriers comparable to those obtained from quantum mechanical methods. The absolute values of the energies are less important, but were also adjusted to improve agreement. The remaining differences in the absolute energy values would primarily effect the temperature scaling in MD simulations.

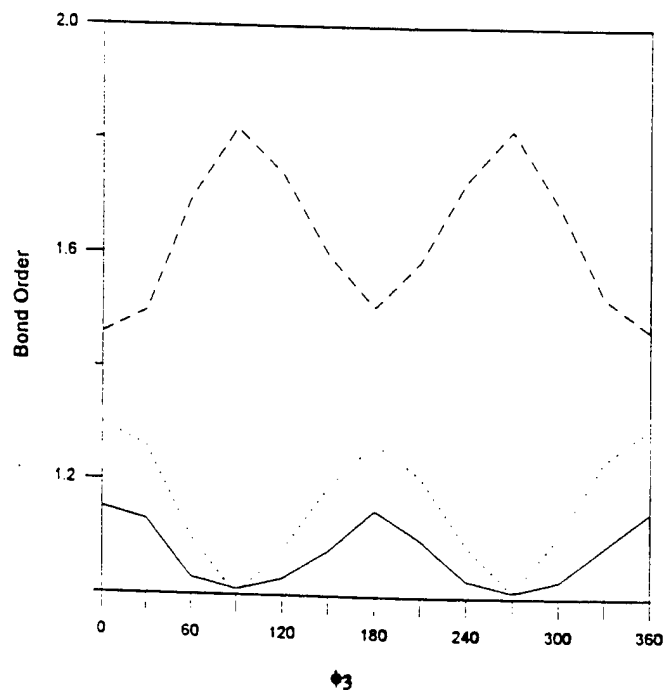


Figure 3.30: Bond orders of bond 1(—), 2(---) and 3(····).  $\phi_1=90^\circ$  and  $\phi_2=180^\circ$ .

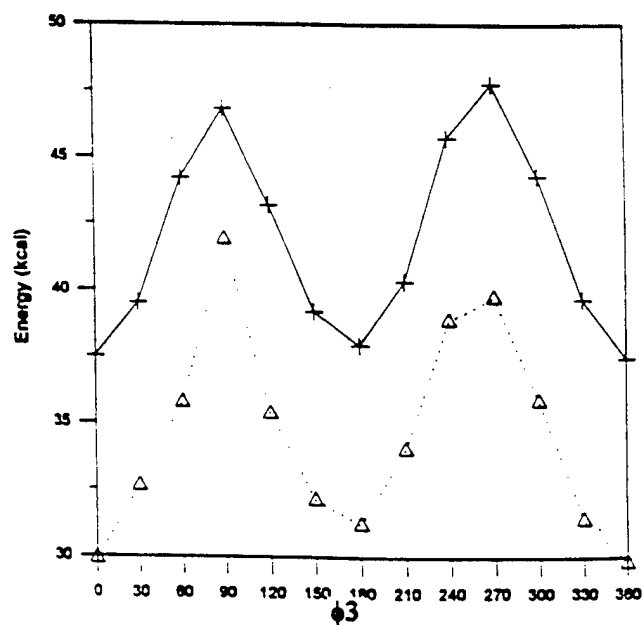


Figure 3.31: Comparison of the energies calculated by the 1-2-1 force field (····) and MOPAC (—).



### Bond Stretching

| Atom i | Atom j | Bond type | $d_{ij}^0$ (Å) | k (kcal/mol Å <sup>2</sup> ) |
|--------|--------|-----------|----------------|------------------------------|
| C2     | C2     | 2         | 1.411 (1.335)  | 700 (1340)                   |
| C2     | C2     | 1         | 1.375 (1.47)   | 1340 (700)                   |
| Car    | Car    | ar        | 1.395 (1.395)  | 700                          |
| C2     | N2     | 1         | 1.357 (1.444)  | 1305.94                      |
| Car    | N2     | 1         | 1.423 (1.346)  | 1305.94                      |
| Car    | Npl3   | 1         | 1.481 (1.35)   | 1306                         |
| C2     | Car    | 2         | 1.411 (*)      | 1000                         |
| Car    | O3     | 2         | 1.214 (*)      | 600                          |

### Angle Bending

| Atom i | Atom j | Atom k | Theta        | k(kcal/moldeg <sup>2</sup> ) |
|--------|--------|--------|--------------|------------------------------|
| C2     | C2     | C2     | 128 (121.7)  | 0.018                        |
| C2     | C2     | Car    | 125 (120)    | 0.026                        |
| C2     | C2     | N2     | 130 (120)    | 0.024                        |
| C3     | C2     | N2     | 109 (118)    | 0.02                         |
| C2     | C3     | Car    | 102 (109.47) | 0.018                        |
| C3     | Car    | Car    | 109 (120)    | 0.024                        |
| Car    | Car    | N2     | 110 (120)    | 0.04                         |
| C2     | N2     | C3     | 124 (110)    | 0.082                        |
| C2     | N2     | Car    | 109 (123)    | 0.08                         |
| *      | C2     | H      | 120 (120)    | 0.024 (0.012)                |

### Torsional

| Atom i | Atom j | Atom k | Atom l | Bond type | k(kcal/mol deg <sup>2</sup> ) | s  |
|--------|--------|--------|--------|-----------|-------------------------------|----|
| *      | C2     | C2     | *      | 2         | 4 (12.5)                      | -2 |
| *      | C2     | C2     | *      | 1         | 9.5<br>(1.424)                | -2 |
| *      | C2     | Car    | *      | 2         | 4 (12.5)                      | -2 |

\* denotes wildcard entries.

Table 3.11: Modified TRIPOS 1-2-1 force field parameters. Values in parentheses are the original TRIPOS values.

The 2-1-2 and 1-2-1 force fields provide reasonable parameterizations for the unsubstituted indoline-benzopyran merocyanine. Are they applicable to substituted indoline-benzopyrans or to benzothiazoline-benzopyran systems? If molecular orbital calculations indicate that the molecules have similar geometric characteristics (angle bending and torsion angles) and electronic characteristics (bond orders), then the modified force fields should be suitable for these molecules as well. The unsubstituted benzothiazoline-benzopyran merocyanine has the same bond orders as the unsubstituted indoline-benzopyran. The average difference in torsion angles between these two molecules is  $1.57^\circ$ . Thus the torsional parameterization should be applicable to either molecule. The measured bond angles differ by an average of  $2.4^\circ$ . The  $C_{18}-C_{17}-C_8$  angle and its counterpart the  $C_{10}-C_9-S_8$  angle ( $109.05^\circ$  and  $116.82^\circ$  respectively), are correctly modeled by the force fields because of their respective equilibrium values of  $109^\circ$  and  $120^\circ$ . The same holds for the  $C_{17}-C_8-C_7$  angle and its counterpart the  $C_9-S_8-C_7$  angle ( $101.82^\circ$  and  $94.41^\circ$  with equilibrium values of  $102^\circ$  and  $97^\circ$  respectively). Thus the modified force fields should be applicable to either the unsubstituted indoline-benzopyran or the unsubstituted benzothiazoline-benzopyran system. A complete investigation of the specific molecule in question is always needed to check the validity of the force field.

### 3.2.2 Molecular Dynamics

Through molecular dynamics, the stability of the chromophore can be studied as a function of molecular environment. The Molecular Silverware algorithm in SYBYL was used to build the solvent-solute system by droplet solvation.<sup>40</sup> This algorithm introduces solvation by successively adding shells of solvent molecules (water, chloroform or ethanol) to the solute (the minimized merocyanine) such that the proper density of the

solvent is maintained. Figure 3.32 shows one such system, the indoline-benzopyran merocyanine in water. Using either the 2-1-2 or 1-2-1 force field along with MOPAC charges (for both the solvent and solute molecules) in the dynamics simulation allows the effect of molecular environment to be studied.

Molecular dynamics simulations consist of two stages, a heating period and an equilibration/simulation period. A gradual heating period was used to minimize the amount of solvent evaporation that occurred (other methods of eliminating vaporization are currently under study). Specifically, the system was heated in 25 K steps lasting 1 ps each. The equilibration/simulation period then lasted for 50 ps at 300 K. Data were obtained every 0.1 ps after sufficient time had elapsed to allow the total energy of the system (potential + kinetic) to remain constant, approximately 20 ps. After equilibrium was achieved, the dihedral angles of bonds 1, 2, and 3 ( $\phi_1$ ,  $\phi_2$  and  $\phi_3$ ) were measured for each of the conformations which arose during the simulation. The standard deviation of each dihedral angle was then calculated in order to quantify the stability of the merocyanine.

The molecular dynamics procedure outlined above can be used to examine the effect of solvent polarity of the solvent on the stability of the merocyanine. Simulations considered systems having solvent polarity of 0 (vacuum), 1.01 D (chloroform), 1.79 D (ethanol) and 1.84 D (water). Results show that as the polarity of the solvent increases, the standard deviation of the dihedral angles decreases (figure 3.33). This suggests that by placing the chromophore in polar solvents the amount of time which the chromophore spends in the planar merocyanine form is increased (i.e. the fading rate will decrease), as is seen experimentally.

In future work it will be necessary to eliminate solvent evaporation. Maintaining the proper density of the solvent will allow both the steric and electronic associations between the solvent and solute to be examined. Due to the large amount of evaporation, only the effect of the polarity of the solvent is seen. Once a more complete force field is

developed (one that changes with torsion angle to account for the bond order changes) the open/closed transition will be modeled.

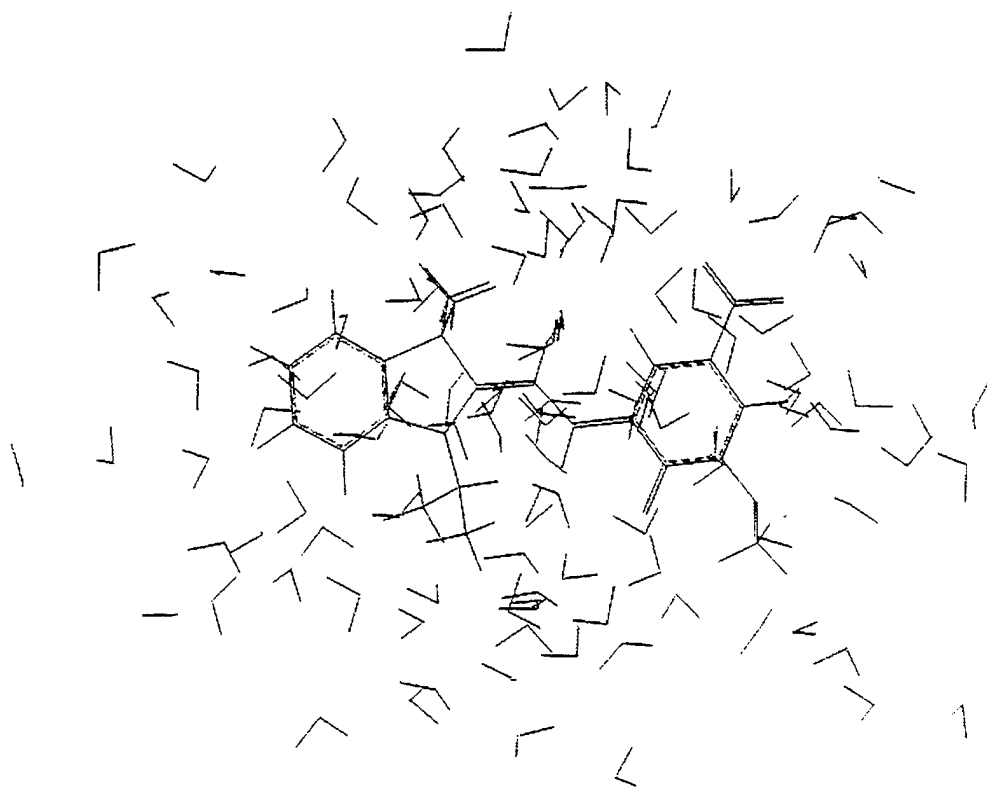


Figure 3.32: The indoline-benzopyran merocyanine in water.

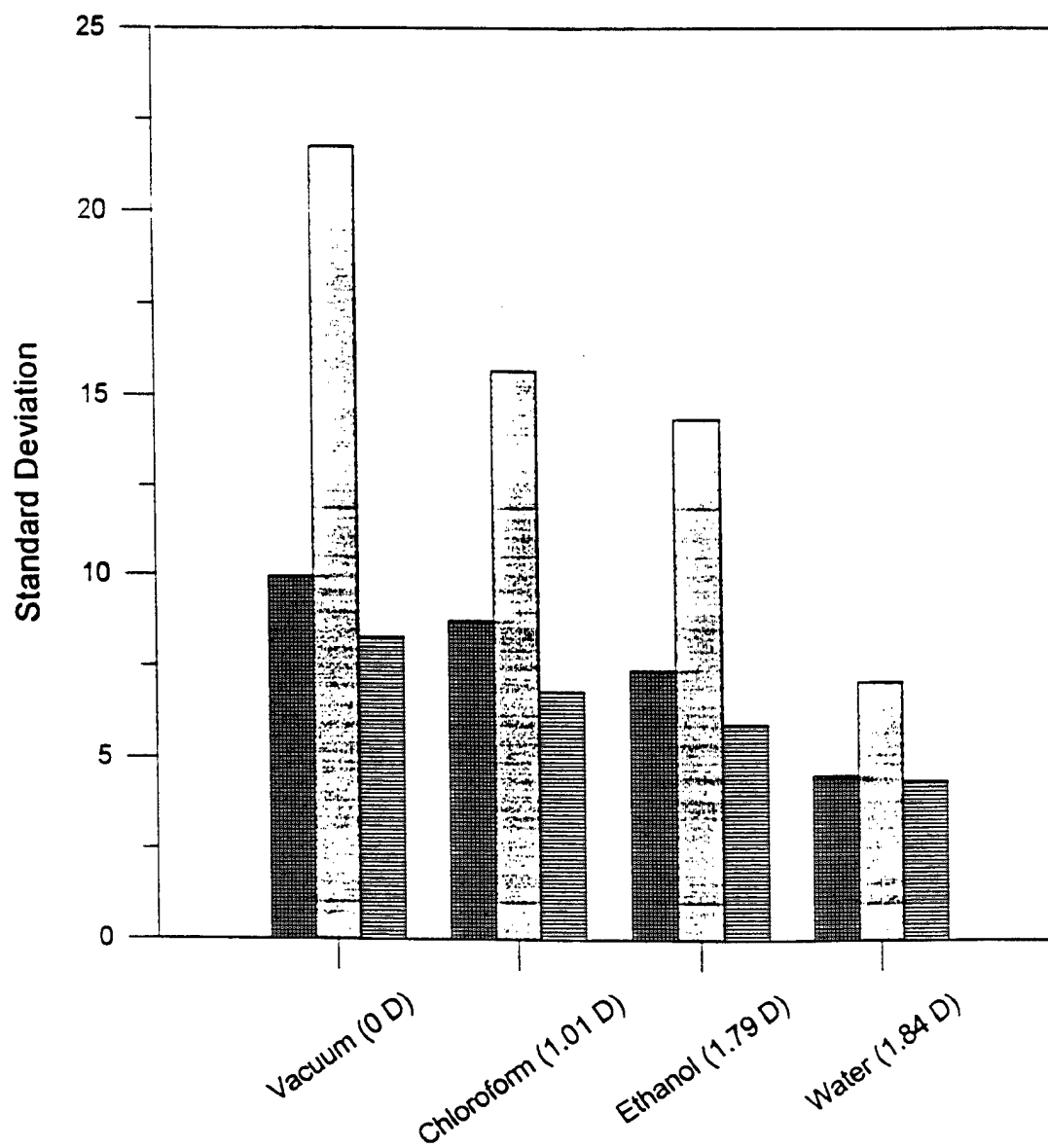


Figure 3.33. The stability of the merocyanine in various solvents (2-1-2 force field).

$\phi_1$  ■■■,  $\phi_2$  □□□, and  $\phi_3$  ▨▨▨ .

## Section IV

### CONCLUSION

"Excellent structure-property correlations might be found for the first five compounds chosen for study: the next five might completely shatter the correlations. Anyone possessing a large collection of spiropyrans can usually play the devil's advocate to proposed theories of photochromism and find compounds whose behavior is much different from that predicted. Conversely, a judicious choice of materials could give experimental support to almost any prediction."

by Bertelson <sup>41</sup>

#### 4.1 Conclusion and Future Directions

The inability to make broad all encompassing statements in the field of photochromism emphasizes the need to investigate chromophores separately and thoroughly. Computational chemistry techniques have been used in this research to probe the structure-property correlations of indoline-spiro-benzopyran and benzothiazoline-spiro-benzopyran. Quantum mechanical techniques were used to obtain the molecular geometries, charge distributions, and most importantly, the electronic spectra. Classical calculations have been used to understand the structure of the chromophore in various solvents at room temperature.

Spectroscopic calculations of the indoline-spiro-benzopyran and the benzothiazoline-spiro-benzopyran have been done. These chromophores (both unsubstituted and substituted) have been considered in both spiropyran and merocyanine

forms. Spectroscopic calculations reveal that the electronic absorption spectra are determined by two factors: the choice of substituent and the geometry of the chromophore. Maximum bathochromic shifts may be achieved in the merocyanine by using strongly electron donating substituents (placed at the proper position) which force rotation about double bonds while limiting the rotation about single bonds. Computational techniques allow the efficient sampling of large numbers of substituted chromophores

Force field calculations are essential in order to model large scale systems (chromophore-solvent interactions and polymer substituted chromophores). In order to correctly model the specific chromophore of interest, two force fields have been developed by altering the TRIPOS force field parameters. These force fields, the 2-1-2 and the 1-2-1 force fields, are the first step toward a classical description of the potential energy surface of the merocyanine. The agreement of the results obtained with these classical force fields and quantum mechanical methods for the unsubstituted indoline-benzopyran merocyanine has been shown. The modified force field parameters were used in molecular dynamics simulations of the indoline-benzopyran merocyanine in order to explore the effect of the environment on the chromophore. These calculations demonstrated the ability of polar solvents to stabilize the merocyanine form, thus potentially reducing the fading rate of the chromophore. Limiting solvent evaporation will allow more qualitative calculations to be done.

These calculations complement each other in the quest to develop efficient chromophore based optical devices. Quantum mechanical calculations have the advantage of being able to calculate the optical properties of the chromophore, yet are limited to small molecules (polymer substituted and solvated chromophores are beyond its capabilities). Meanwhile, classical calculations yield information about the time averaged structural behavior of polymer substituted and solvated chromophores but are unable to account for any chemical changes in the system. It has been demonstrated that

correlations may be made between the structure of indoline and benzothiazoline spiro-benzopyran chromophores (both by choice of substituent and bond twisting) and their optical properties.

The accurate modeling of both the closed/open transition and the interconversion between isomers of the merocyanine require force fields that are capable of properly accounting for the chemical changes which occur. This can be done by allowing the force field to be a function of the important characteristics of the molecular geometry such as the sequence of bond orders. Relative transition rates could then be calculated as functions of molecular environment, pressure and temperature. Because the optical spectrum is a function of the chromophore's geometry, the time/temperature averaged structural information that molecular dynamics provides may then be used to predict the spectral properties of the system.

Computer aided simulations offer a deeper understanding of both the optical and the structural properties of the indoline-spiro-benzopyran and the benzothiazoline-spiro-benzopyran. As fundamental scientific and commercial interest in the photochromic process continue to be expressed, exciting possibilities lie ahead for improvements to existing chromophore based devices and the invention of the devices of the future.



## REFERENCES

- 1 Guglielmetti, R., 'Photochromism: Molecules and Systems', Elsevier Science Pub. Co., New York, 1990, 314
- 2 Kholmanskii, A.S. and Dyumaev, K.M., *Russian Chemical Reviews* 1987, **56** (2), 136
- 3 Ibid., 314
- 4 Kholmanskii and Dyumaev, 143
- 5 Bertelson, R., 'Photochromism' (Ed. Brown, G.), J. Wiley and Sons Inc., New York, 1971, 98
- 6 Ibid., 98
- 7 Ibid., 50
- 8 Guglielmetti, 337
- 9 Ibid.
- 10 Ibid., 326
- 11 Bertelson, 117

- 12 Ibid., 171
- 13 Ibid., 117
- 14 Ibid., 735
- 15 Ibid., 744
- 16 Private communication from Martin C. Baruch to Jennifer A. Young, February 5, 1993
- 17 Schatz, G., and Ratner, M., 'Quantum Mechanics in Chemistry', Prentice-Hall, Inc., Englewood Cliffs, New Jersey 1993, 145
- 18 Ibid., 135
- 19 Suzuki, H., 'Electronic Absorption Spectra and Geometry of Organic Molecules', Academic Press, New York, 1967, 179
- 20 Schatz and Ratner, 17
- 21 Ibid., 145
- 22 SYBYL Molecular Modeling Software: Version #6.0, Tripos Associates, Inc., St. Louis, 1992, 2140

- 23 Schatz and Ratner, 144
- 24 Ridley, J., and Zerner, M., *Theoret. Chim. Acta.* 1973, **32**, 112
- 25 Schatz and Ratner, 124
- 26 Suzuki, 64
- 27 Gilbert, A., and Baggott, J., 'Essentials of Molecular Photochemistry',  
Blackwell Scientific Publications, Boca Raton, Florida, 1991, 85
- 28 Clark, M., Cramer, R., and Van Opdenbosch, N., *Journal of Computational  
Chemistry* 1989, **10**, 982
- 29 Suzuki, 88
- 30 Ridley and Zerner, 112
- 31 Tinland, B., Guglielmetti, R., and Chalvet, O., *Tetrahedron* 1973, **29**, 666
- 32 Pachter, R., Cooper, T., Natarajan, L., Obermeier, K., Crane, R., and Adams,  
W., *Molecular Dynamics Simulatoin of Poly(Spiropyran-L-Glutamic-  
Acid): The Influence of the Chromophore Conformation*, 6
- 33 Gilbert and Baggott, 86

- 34 Kholmanskii, A., Zubkov, A., and Dyumaev, K., *Russian Chemical Reviews* 1981, **50** (4). 306
- 35 Guglielmetti, 315
- 36 Kholmanskii and Dyumaev, 139
- 37 Suzuki, 134
- 38 Ibid.
- 39 Zumdahl, S., 'Chemistry', D.C. Heath and Company, Lexington, 1986, 300
- 40 SYBYL Molecular Modeling Software: Version #6.0, Tripos Associates, Inc., St. Louis, 1992, 1129-1
- 41 Bertelson, 99